Caged oxoanions†

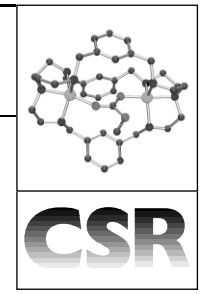

Vickie McKee,[a] Jane Nelson[bc] and Raewyn M. Town[c]

[a] *Chemistry Department, Loughborough University, UK LE11 3TU*
[b] *Biomedical Science, University of Ulster, Coleraine, UK BT52 1SA*
[c] *School of Chemistry, Queen's University Belfast, Belfast, UK BT9 5AG*

Received 27th February 2003
First published as an Advance Article on the web 14th July 2003

The association between azacryptand hosts and oxoanion guests is reviewed. Positively charged hosts are the most effective; we focus on protonated azacryptands. Assessment of quantitative data suggests an anion cryptate effect and provides clear evidence for charge-based selectivity. Crystal structures show both cavity and cleft binding sites for anions within the series of cryptands studied. These two binding modes exhibit different pH dependence, offering the possibility for design of monitoring/clean-up strategies based on a variation of appropriate host(s) and pH conditions.

All the authors have been associated over the years with Belfast and with New Zealand. Jane Nelson, although not on the staff of QUB, carried out research in an honorary capacity from that base for over 30 years. She is currently affiliated to University of Ulster, and is grateful for provision of facilities there which enable continuation of her research. Much of her contribution to this review was written while in the University of Canterbury, NZ, under the auspices of an Erskine Visiting Professorial Fellowship. Vickie McKee also initiated her research career in Belfast under Martin Nelson's supervision, left for a post-doctoral fellowship with Chris Reed in California followed by 11 years on the staff of University of Canterbury, and having circumnavigated the globe, returned to Belfast in 1993. She was attracted to Loughborough as Professor and Head of Inorganic Chemistry in 2001. The third member of the group, Raewyn Town, started off on the other side of the globe, with PhD research at the University of Canterbury under Kip Powell's supervision. She then undertook postdoctoral research with Jacques Buffle at the University of Geneva, followed by a brief stint on the staff of Massey University, New Zealand, before taking up her current post at QUB in 1995.

V. McKee R. M. Town J. Nelson

† Electronic supplementary information (ESI) available: tables of protonation and stability constants and graphs of species formation as a function of pH for R3Bm + malonate and R3P + malonate and the distribution of protonated species as a function of pH for Me_6R3Bm. See http://www.rsc.org/suppdata/cs/b2/b200672n/

1 Introduction

The cryptand ligands developed by J.-M. Lehn over 30 years have now comprehensively illustrated the brilliance of his original strategy: replacement of the solvent shell of a cation by a preformed three dimensional cage ligand or "cryptand" to enhance both thermodynamic and kinetic stability of the product.[1] These cryptands when positively charged, as for example by protonation at nitrogen, have proved also to have useful properties in anion encapsulation.[2,3] The challenges posed in anion encapsulation are more testing than those faced in cation encapsulation, given the weaker host–guest interaction, larger and more variable shape and the greater lability of anions *versus* cations, as well as the stronger competition faced from solvation or hydration equilibria. Monitoring of success in this area, too, poses problems because of the spectroscopic silence of most anions.

Nonetheless the objective of achieving strong and selective complexation of anions is one that is becoming difficult to ignore. There are pressing environmental/biomedical reasons to develop oxoanion complexants for monitoring or sequestration of potentially harmful anions, including highly soluble species such as nitrate, phosphate or aluminate once thought harmless and permitted to accumulate in lakes and rivers, but now known to be deleterious to the environment and in some circumstances possibly also to human health. Oxoanions as a group are characterised by high aqueous solubility, and even the more blatantly toxic examples, such as those of As, Sb, Pb and Cr, present locally in high concentration from industrial or mining activities, are still in need of more effective complexants. Also requiring monitoring and effective control are the accumulating concentrations of $^{188}ReO_4^-$ and $^{99}TcO_4^-$ or other radioactive anions generated in consequence of radiopharmaceutical use and/or in the nuclear industry.

Nor does the interest in anion complexation rely solely on the need to monitor and remove pollutants. Anion reactivity is a topic of importance;[4] the majority of enzyme substrates are anionic, and any replication of their catalysed reactivity under mild biological conditions, using synthetic hosts, represents a useful advance.

For all these reasons the objective of meeting the challenges inherent in anion, particularly oxoanion, complexation is worthwhile, and warrants the degree of attention it is starting to attract. Many isolated studies of cleverly designed receptors capable of complexing and reporting on particular target anions have been carried out.[5] Elegant organic synthetic procedures have been developed and detailed structural studies achieved. However, in all this, the necessary physicochemical studies of

thermodynamics and kinetics of complexation have perhaps been underaddressed, given that the field is by now reaching the mature stage where quantitative data can be of considerable value in systematising the principles governing interaction.

The most effective hosts for anions are expected to be positively charged, so both dinuclear cation cryptates and protonated azacryptands are potential hosts for anion uptake and complexation studies. There is a not-unreasonable expectation that the existence of an "Anion Cryptate" effect analogous to that now widely accepted for cations may be established.

1.1 Early oxoanion cryptates

Anion complexation has attracted sporadic attention since the early days of cryptand chemistry. The first cryptand synthesised (I: Fig. 1) was isolated[6] as a hydrochloride salt; X-ray crystallography eventually demonstrated encapsulation of the chloride anion. An all-aza N_4 macrotricycle with hexamethylene chain spacer length (Fig. 1: II) synthesised by Schmidtchen[7] was later shown to encapsulate dihydrogenphosphato-, acetato- and hydrogencarbonato anions with complexation constants which were relatively large (log K values of 2.1, 1.86, and 1.76 respectively) given that interactions with these quaternary nitrogen hosts are mainly restricted to electrostatic. However the most extensive series of complexation parameters obtained in early studies with azacryptand hosts involved the systems O-bistren (trisethyleneamino-derived caps and bisethyleneoxo straps) and the more basic ligand C3-bistrpn (trispropyeneamino-derived caps and trismethylene straps); Fig. 2. These cryptands when hexa- (O-bistren) or octa- (C3-bistrpn) protonated show[2] large complex formation constants log K_{app}‡ (of the order of 5–10) for multiply charged (Table 1) oxoanions and values smaller by at least 3 log units for singly charged anions such as hydrogencarbonate or nitrate (log K_{app} values for the O-bistrenH_6^{6+} host are 2.3 and 2.8 respectively). The indications are thus present of both charge- and shape-based selectivity. However, no crystal structures are available for oxoanion cryptates of this series, which restricts consideration of the non-covalent interactions such as hydrogen-bonding or hydrophobic interactions. The Lehn group also developed barrel-ended cryptand hosts[8] deriving from 1,3,5 tris benzylamine caps (Fig. 1: III and IV) for which approximate complexation constants were estimated. These protonated hosts demonstrate better complexation properties for dinegative anions (log Ks in the range 5–6.5) than for mononegative ones (log Ks in the range 2.5–4), though the extent to which this preference may be based in steric factors is again impossible to decide because of the absence of structural data. An X-ray crystal structure (Fig. 3) is however available to illustrate the relationship between host and terephthalate guest[9] in an aromatic (diphenylmethane-linked) host. The relatively large complexation constant observed derives from good steric complementarity of the host/guest combination as well as extended H-bonding of terephthalate within the crystal lattice, rather than on any specific π–π interaction.

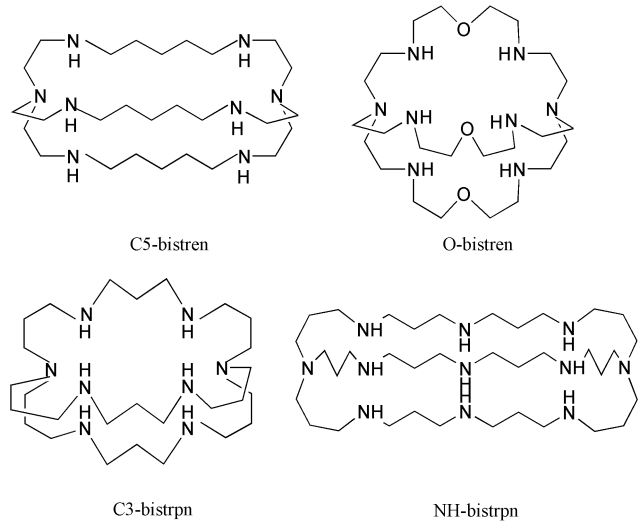

Fig. 2 Macrobicyclic cryptate hosts for anions: O-bistren, C3-bistrpn, C5-bistren, NH-bistrpn.

1.2 Positively charged azacryptate hosts: *via* the [2 + 3] Schiff-base condensation reaction

Some years ago[18] we discovered that the facile Schiff-base condensation reaction could be used in [2 + 3] mode to generate cryptand ligands from triamines and dicarbonyls in high yield under mild conditions in a one-pot synthesis, without the need for high-dilution techniques.

The hexaimine products can be readily reduced with borohydride to generate the more chemically robust aminocryptands. These are basic ligands which we soon realised make good hosts for anions when protonated. The protonation constants for these cryptands in tosylate media (this large poorly H-bonding anion is the notional standard for these studies[2]) are given in the ESI.† Fig. 4 illustrates its location[19] external to the cavity, even in this largest-cavity host of the *tren*-capped series. In the smaller *m*-xylyl-spaced hexaprotonated cryptate host the tosylate ions also surround the macrobicycle to which most of the sulfonate ions are directly linked by hydrogen bonding.[20] As it is not feasible to use a completely non-hydrogen bonding anion for aqueous studies, we have continued to follow established practice and use the tosylate ion as calibrant so that our results are comparable with literature values. The observation that these protonation constants, especially the most acidic ones, are rendered more basic in other electrolytes, including

‡ Log K values are relative to the anion in the supporting electrolyte. In our work we have used tosylate, the notional standard. Units of K are $dm^3\ mol^{-1}$.

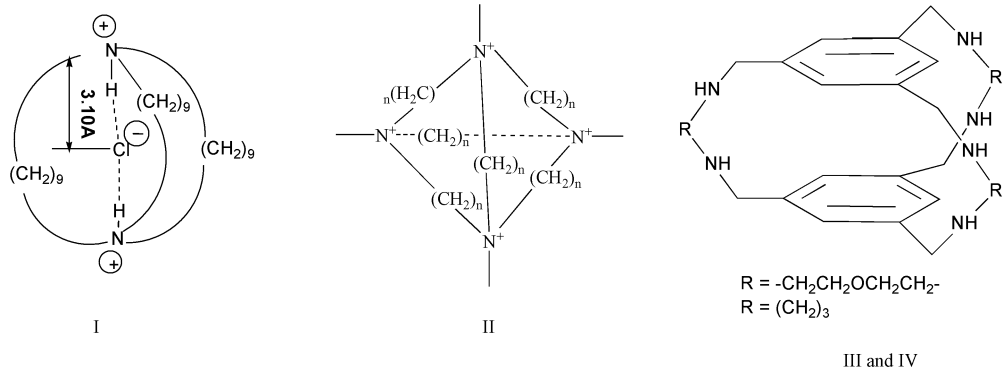

Fig. 1 Macrobicyclic and tricyclic hosts I and II, and Barrel ended cryptate hosts III and IV for oxoanions.

Table 1 Published complexation constants of dinegative oxoanions with N-donor macrocyclic amd macrobicyclic ligands

Ligand	Reaction	Log K/dm^3 mol^{-1}		
		X = sulfate	X = oxalate^{2-}	X = malonate^{2-}
O-bistren[10]	$H_6L + X$	4.90		
	$H_5L + X$	2.90		
C3-bistrpn[11]	$H_8L + X$	7.45	6.55	4.00
	$H_7L + X$	5.60	5.20	3.10
	$H_6L + X$	4.20	4.50	2.85
	$H_5L + X$	3.20	3.25	2.20
	$H_4L + X$	2.75		
[24]aneN6[11]	$H_6L + X$	4.05	3.80	3.30
	$H_5L + X$	3.05	3.20	2.60
	$H_4L + X$	2.50	2.60	2.45
[32]aneN_8[13]	$H_8L + X$	4.0	3.7	3.9
[27]aneN_6O_3[13]	$H_6L + X$	4.5	4.7	3.8
[21]aneN_7[12]	$H_6L + X$	5.42		
	$H_5L + X$	4.05		
	$H_4L + X$	3.03		
	$H_3L + X$	2.34		
	$H_2L + X$	2.2		
1,4,7-triNMe -[21]aneN_7[12]	$H_6L + X$	6.94		
	$H_5L + X$	5.12		
	$H_4L + X$	4.09		
	$H_3L + X$	3.38		
	$H_2L + X$	2.93		
1,5,9,17,21,25-hexaaza[32]ane[14]	$H_6L + X$		3.20	3.8
1,5,9,20,24,28 [38]ane[14]	$H_6L + X$		6.30*	4.05
BFBD (bisfuran bisdien)[15]	$H_6L + HX$			1.86
	$H_6L + X$		4.97	4.01
	$H_5L + X$		4.12	3.39
	$H_4L + X$		2.97	2.10
O-BISDIEN ([24]ane-N_6O_2)[16,17]	$H_6L + HX$			2.2
	$H_6L + X$		4.68	4.2
	$H_5L + X$		3.59	3.70
	$H_4L + X$		2.06	2.38
	$H_3L + X$			2.05
	$H_2L + X$			1.81

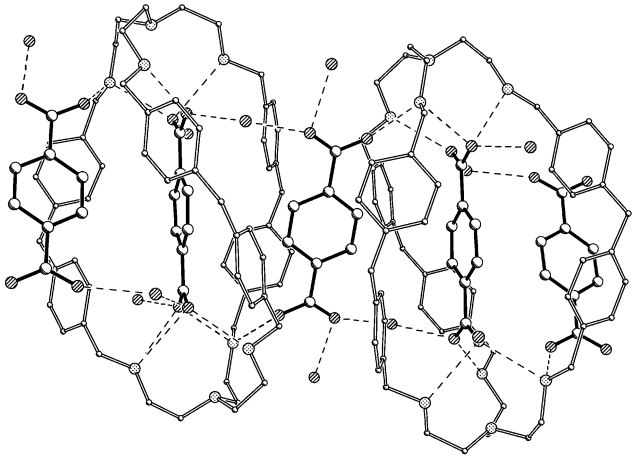

Fig. 3 Terephthalate anions bound within a diphenylmethane-linked host. The individual cryptates are linked into chains by hydrogen-bonding to unencapsulated terephthalate ions.

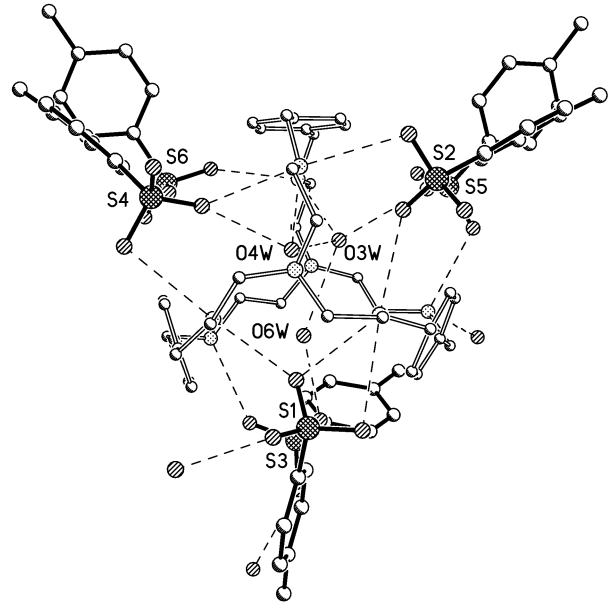

Fig. 4 Tosylate cryptate of R3Bp; showing encapsulation of three water molecules in preference to the large OTs^- anion. All six tosylate ions are cleft-bound *via* hydrogen bonds in the range 2.73–3.03 Å.

the weak H-bond acceptor perchlorate§, provides evidence for stronger association of these anions with the protonated cryptand. The protonation constants in ClO_4^- media are given in the ESI.† The protonation constants of the pyridine-spaced cryptand R3P are unaffected by substitution of perchlorate for tosylate, presumably because neither anion is encapsulated (see Fig. 8).

Our work to date has concentrated on the more readily accessible ligands that are generated in reasonably high yield and purity as free cryptands, *i.e.* R3Bp, R3Bm, R3F and R3P (Scheme 1), analogous to the aliphatic methylene-spaced cryptands generated by Lehn and shown as C5bistren, O-bistren, or NHbistrpn in Fig. 2. The *tren*-capped Schiff-base-derived cryptands R3Bm – R3P are available in a pure form in sufficient quantity and have sufficient aqueous solubility to allow study with a wide range of guests and by more than one technique. Owing to lack of sufficiently pure samples of the *tris*propylene (trpn)-capped free cryptands, we have not attempted any systematic work on that series, although we have obtained[18] the structure of an octaprotonated cleft-bound perchlorate cryptate serendipitously isolated in the course of attempts at cation complexation. Thus from these initial structural studies we were aware of two different binding sites for oxoanion complexation as illustrated schematically in Fig. 5: the encapsulated (as in Fig. 3) and cleft-bound (as in Fig. 4) options.

The choice appears to some extent to be governed by the steric compatibility between oxoanionic guest and protonated host, but we note that some hosts have a pronounced tendency to favour the cleft-binding conformation, and others none at all.

2 Protonated aminocryptate receptors

2.1 Tetrahedral mononegative oxoanions

The first oxoanion cryptate to be isolated with our systems[21] was a perchlorate cryptate obtained in the course of an attempt to generate a dinuclear complex of manganese. The cryptate is

§ Perchlorate was initially and is still occasionally[12] used as supposedly inert ionic medium in anion encapsulation experiments with macrocyclic hosts.

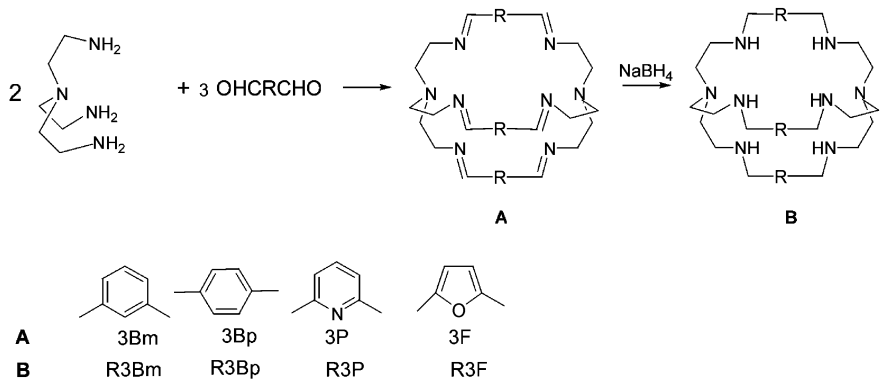

Scheme 1

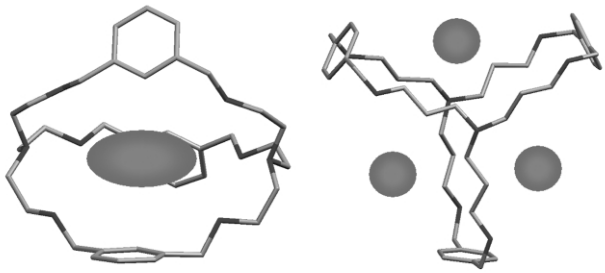

Fig. 5 Schematic illustration of cavity (i) *vs* cleft (ii) modes of cryptand binding.

in the hexaprotonated form and the anion is symmetrically disposed within the cavity (Fig. 6). Disorder (involving 180° reversal of the ClO bond aligned with the $N_{bridgehead}$–$N_{bridgehead}$ axis) to some extent obscures the details of the hydrogen-bonding interactions but it is clear that both direct NH^+–$O_{perchlorate}$ and indirect NH^+–O_{water}–$O_{perchlorate}$ hydrogen bonds contribute to the stability of the complex. (Six of the nine water molecules are located in interstrand clefts, and act as H-bond bridges between NH^+ and $O_{oxoanion}$).

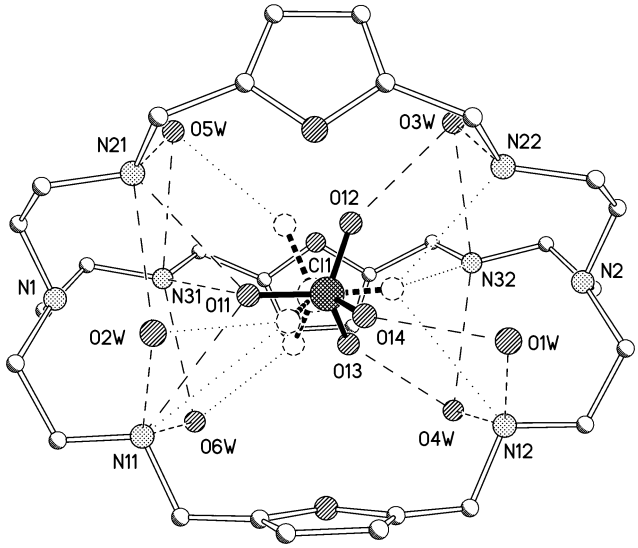

Fig. 6 Perchlorate cryptate of H_6R3F^{6+}. The central perchlorate anion is disordered over two equivalent orientations. O11 is directly hydrogen-bonded to the cryptate while O12, O13 and O14 are indirectly hydrogen-bonded to the amines (*via* water molecules). Selected hydrogen bond distances: O11–N11, 3.06(2); O11–N21, 3.09(2); O11–N31, 3.19(2); O12–O3W, 2.74(2); O13–O4W, 2.76(2); O14–O1W, 2.91(2); O1W–N12, 2.79(9); O2W–N11, 2.78(9); O3W–N22, 2.83(1); O4W–N32, 2.93(1); O4W–N12, 3.12(1); O5W–N21, 2.85(1); O6W – N31, 2.89(1) Å.

This combination of direct and indirect hydrogen-bonding recurs in structures of products later synthesised intentionally *via* treatment of the tetrahedral oxoanion with the cryptand host under conditions of low pH. A typical anion cryptate structure is that shown in Figure 7. The protonated cryptand $[R3BmH_6]^{6+}$

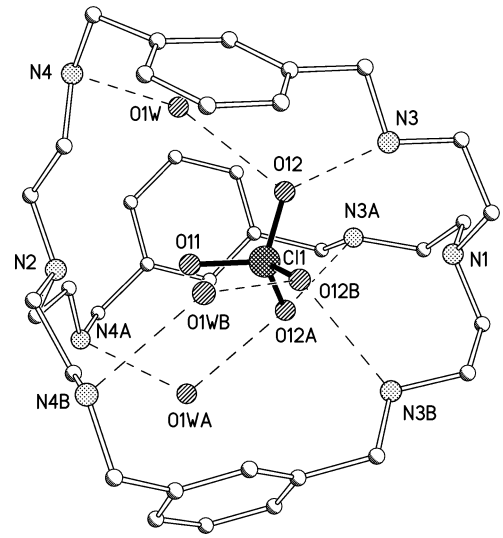

Fig. 7 Perchlorate cryptate of R3Bm H_6^{6+}. The anion is encapsulated *via* three direct and three indirect hydrogen bonds: N3–O12, 2.790(5); N4–O1W, 2.712(6); O1W–O12, 2.782(5) Å (the complex has 3-fold symmetry).

acts as host for a perchlorate guest which is hydrogen-bonded to three symmetry-related amines at one end of the cage and indirectly to the set of amines from the other end *via* water molecules from the remnant hydration sphere. The perchlorate oxygen atom lying on the 3-fold axis does not appear to be involved in hydrogen-bonding but is surprisingly close (2.559(4) Å) to the bridgehead nitrogen atom. The relatively strong hydrogen-bonding network involving the three bridging water molecules is responsible for the unsymmetric pear-shape of the host. We will see that the combination of direct amino-anion $NH^+\cdots O^-$ hydrogen-bonding and indirect bridging *via* remnant hydration shell molecules[22] observed here is a recurring motif in oxoanion cryptate structures.

A third structure involving perchlorate in this group is seen in the octaprotonated pyridine-spaced cryptand host R3P (Fig. 8). Here[23] the crypt fails to adopt an inclusive structure, opting instead for a version of the cleft-binding conformation exhibited in the free ligand[19] (Fig. 9). Each amino nitrogen is hydrogen-bonded to one oxygen on each of two ClO_4^- anions on either side of the strand and water molecules, some quite strongly H-bonded, facilitate further hydrogen-bonding interactions between ClO_4^- oxygen atoms. Protons are located on two of the three pyridine nitrogens¶ and these protons, located by X-ray

¶ Although pyridine N-donors are capable of protonation at low pH, as demonstrated here, we have not seen evidence of their protonation in solution in these systems.

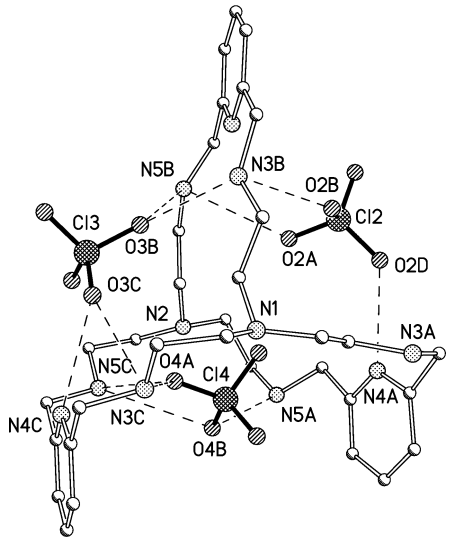

Fig. 8 Cleft binding conformation utilised in R3P H_8^{8+}. Selected H-bond distances: N4A–O2D, 2.755(4); N5A–O4B, 2.915(4); N3B–O2B, 2.829(4); N3B–O3B, 2.974(3); N5B–O2A, 2.998(4); N5B–O3B, 2.976(4); N3C–O4A, 3.121(4); N3C–O3C, 2.956(3); N4C–O3C, 2.991(4); N5C–O4A, 3.168(4); N5C–O4B, 3.125(4) Å. For reasons of clarity, only the 3 cleft-bound perchlorates are shown and binding of water molecules is not illustrated.

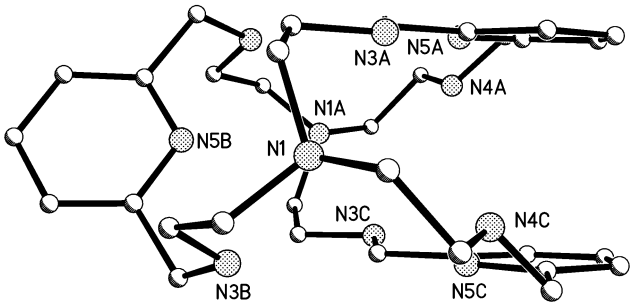

Fig. 9 Cleft conformation in free cryptand R3P showing π–π interaction between the pyridine rings containing N5A and N5C; centroid of one ring lies 3.69 Å from the mean plane of the other.

crystallography, form hydrogen bonds to perchlorate oxygens. The relatively open cleft-binding conformation is found, as we will see, in other R3P cryptates. In contrast, the R3Bm and R3F hosts, whether protonated or not, opt in general for cavity-binding conformations.

The tetrahedral mononegatively charged radioactive oxoanion perrhenate $^{188}ReO_4^-$ is of medical interest[24] in connection with specific therapeutic and diagnostic applications, where direct complexation upon generation of the radioisotope is highly desirable. Stable isotopic forms of ReO_4^- are also of interest as models for the behaviour of the radioactive oxoanion $^{99m}TcO_4^-$ which is widely used in diagnostic medicine. $^{99}TcO_4^-$ is additionally a long lived and hazardous component of nuclear effluent. Perrhenate is readily encapsulated by the hexaprotonated azacryptand host R3Bm (Fig. 10). In this

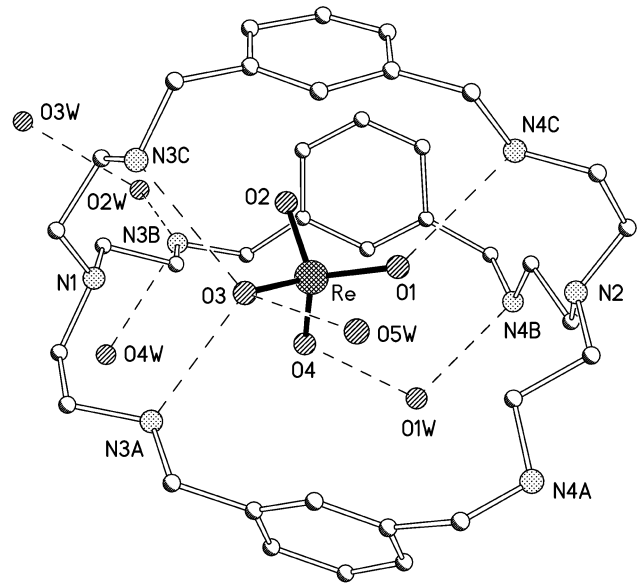

Fig. 10 Perrhenate cryptate of R3Bm H_6^{6+}. Selected H-bond distances: N3A–O3, 2.99(2); N4B–O1W, 2.698(19); N3B–O2W, 2.85(2); N3B–O4W, 2.90(2); N3C–O3, 2.938(18); N4C–O1, 2.862(19); O1W–O4, 2.86(2); O2W–O3W, 2.82(2); O5W–O3, 3.13(2) Å.

$[R3BmH_6(ReO_4)]^{5+}$ cryptate, both ends of the crypt participate in direct and indirect intramolecular (water-mediated) H-bonding, although not all the NH^+ protons H-bond intramolecularly. Notwithstanding the similarity with the perchlorate structure, syntheses of mixed perrhenate/perchlorate cryptates carried out with varying stoichiometric ratio of ReO_4^- to ClO_4^- invariably generate[19] the ReO_4^- encapsulated-form.

Once again, complexation of this oxoanion using the pyridine-spaced cryptand R3P is seen (Fig. 11) to generate a cleft-bound[25] rather than encapsulated complex, for the mixed oxoanion formulation $(H_6R3P)_2.(ReO_4)_{10}.(ClO_4)_2.3H_2O$. In this structure there are two crystallographically independent molecules in the unit cell, one involving $[R3PH_6]^{6+}$ with all-perrhenate counteranions and the other a diperchlorate tetraperrhenate of $[R3PH_6]^{6+}$ with perchlorate counteranions in two of the clefts and perrhenate in the third. Inspection of this structure illustrates the structural adaptability of the cleft-binding conformation. Relatively minor alteration of cleft angles

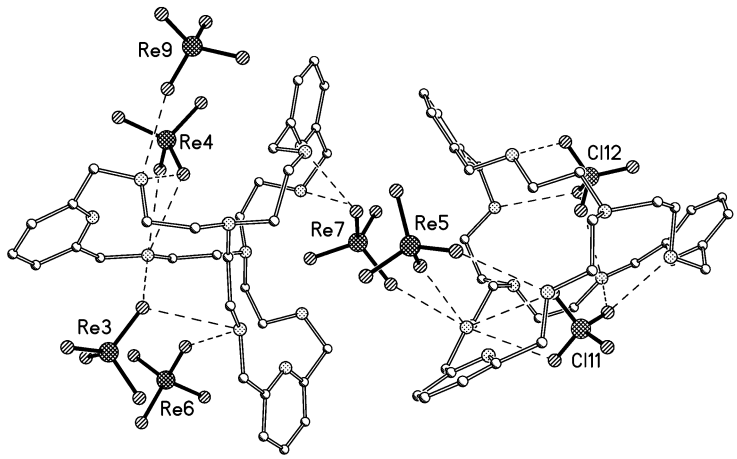

Fig. 11 Perrhenate structure of $R3PH_6^{6+}$ showing cleft binding and bridging anions. Shortest H-bond to perchlorates **11** and **12**: 2.82(1) and 2.83(1); to perrhenates **5**, **4**, **3**: 2.81(2), 2.94(2), 2.85(2) Å.

permits both the larger perrhenate and the pair of smaller perchlorate oxoanions to be neatly accommodated within their respective cleft-sites so that reasonably short H-bonds are available in both cases.

2.2 Trigonal oxoanion encapsulation

While steric compatibility of tetrahedral oxoanions with the trigonal symmetry of the cryptand host in its cavity-binding conformation is clearly an aid to efficient complexation, this is not restricted to tetrahedral guests. In the perchlorate series for example, only the top face of the tetrahedron is involved in H-bonding, albeit to both upper and lower sets of three NH^+ donors. So it was no surprise to discover that nitrate is also efficiently encapsulated by these cryptand hosts.

What was a surprise however was the discovery[26,27] that not one, but two nitrate anions are encapsulated in the solid state, as the crystal structure (Fig. 12) shows. As in the case of perchlorate each oxoanion O is chelated by a pair of NH^+ donors so each nitrate anion is tethered by 6 direct H-bonds; each NH^+ makes a pair of bifurcated H bonds to adjacent nitrate oxygen atoms. Given that both sets of protonated N-donors are occupied in direct H-bonding, there is no opportunity for the indirect, intramolecular water-mediated H-bonds which play an important role in stabilising encapsulated MO_4^{n-} anions. There are externally directed water-mediated H-bonds tethering extracavity nitrate anions which are the shortest H-bonds (2.66, 2.73, 2.77 Å) in the structure. The hydrogen-bonded network (Fig. 13) involved in retention of these external nitrate anions runs through the whole structure apart from areas occupied by aromatic rings, as seen earlier in the structure shown in Fig. 3.[9] The possibility that solid state and solution complexation behaviour might not be identical in these systems drew attention to the necessity for quantitative solution complexation studies.

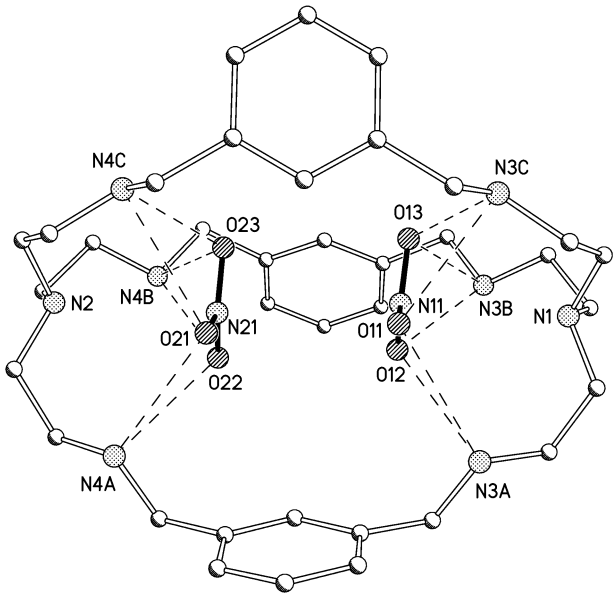

Fig. 12 Dinitrate cryptate of $R3BmH_6^{6+}$. Cryptate cation, showing intramolecular H-bonds selected distances: N3A–O11, 2.8819(15); N3A–O12, 3.0244(15); N4A–O21, 2.8415(14); N4A–O22, 2.9882(15); N3B–O12, 2.8384(16); N3B–O13, 3.0386(16); N4B–O22, 2.8595(15); N4B–O23, 3.0350(16); N3C–O13, 2.8781(16); N3C–O11, 2.9518(15); N4C–O23, 2.8968(16); N4C–O21, 2.9814(15); N11–N21, 3.391(1) Å.

2.3 Quantitative solution measurements: mononegative oxoanions

Both pH-potentiometry and NMR shifts can be used in the case of the relatively weak-binding mononegative oxoanion systems to measure complexation constants. The program EQNMR[28] was used in conjunction with ^1H NMR shifts at pH 3, where the cryptand hosts are known[19,29] to exist in the hexaprotonated state. This allows complexation to be monitored as a function of oxoanion concentration in tosylate supporting electrolyte. For nitrate, at relatively low oxoanion to cryptand ratios, good fit with experimental data was obtained for a simple model of 1:1 complexation with log K_{app} values of the order of 3–4.[19,25,27] It was only in the presence of a very large excess of nitrate that there was some evidence for formation of a 2:1 species in solution. However, only small fractional log K_2 $H_6LNO_3^{5+}$ + NO_3^- values (for the host $R3BmH_6^{6+}$: K_2 = 1.87 ± 0.73 dm^3 mol^{-1}) could be evaluated for this second equilibrium.

Complexation constants were also estimated by analysis of the results of pH-metric titrations carried out in the presence of target anion (with the large size-excluded ion tosylate as the supporting electrolyte). As noted above (Section 1.2), the alteration in K values in the various media used reflects the contribution of anion complexation to the equilibria. The individual ligand–anion association constants were evaluated from these data by fixing the protonation constants at the values determined in tosylate medium and including an additional constant for 1:1 ligand:anion association in the refinement, for the various levels of ligand protonation. Comparable values were obtained by both NMR (at pH 3) and pH-potentiometric methods over the range 3 to 11 for mononegative oxoanions with protonated R3Bm, R3F and R3P hosts.[19,25,27]

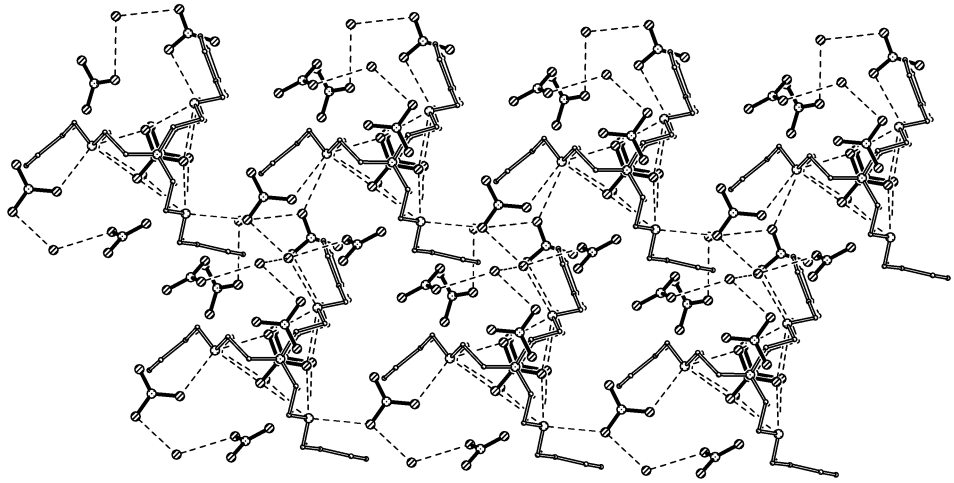

Fig. 13 Dinitrate cryptate of $R3BmH_6^{6+}$. Lattice showing intermolecular H-bonds involving extracavity nitrate ions.

The 1:1 nitrate-binding constants for R3Bm and R3F (log K_{app} 2.80 dm^3 mol^{-1}) are around an order of magnitude higher than that measured under similar conditions[30] for nitrate association with O-bistrenH$_6^{6+}$. For perchlorate, despite its weak hydration, no complexation constants sufficiently large to be quoted with confidence have been obtained elsewhere using cryptand hosts§. From this it may be inferred that the values for nitrate which, although small, are large enough to be relied upon, lie in general above those for perchlorate complexation.

In the series of azacryptand ligands of Scheme 1, it is generally noted that the furano-linked host R3F, which reliably operates as a cavity-binding host for oxoanions, exhibits lower binding constants than does the *m*-xylyl linked host R3Bm. This may be attributed to the lower basicity of the heterocycle-incorporating cryptand (overall Σ log K_i = 43.46 for R3F and 46.76 for R3Bm at the hexaprotonated level *vs* 52.35 at hexaprotonated level and 61.45 at octaprotonated level for C3-bistrpn[11] and 47.90 at hexaprotonated level for O-bistren[10]). This parameter also puts the basicity of R3Bm below that of O-bistren and especially C3-bistrpn or all-methylene linked bistrien macrocyles, (Σ log K_i for the heptamethylene version = 54.35[14]) but well above those of protonated hexaaza heteroatom linked macrocyclic ligands such as O-bisdien[16,17] and its furano-bridged analogue BFBD[15] (Σ log K_i = 41.58 and 39.23, respectively) whose quantitative complexation properties for oxoanions have been measured.[15] The pyridine-linked host R3P shows similar basicity to R3Bm with an overall Σ log K_i of 45.36 although the tendency of R3P to adopt a cleft- rather than cavity-binding conformation complicates comparison with encapsulating hosts such as R3F and R3Bm. This tendency is once more illustrated in the nitrate complex of R3P, where a nitrate anion intercalates 3.3 Å distant from each of the approximately parallel pyridine rings which terminate the cleft. (Fig. 14). Interestingly, this structure also illustrates, in two

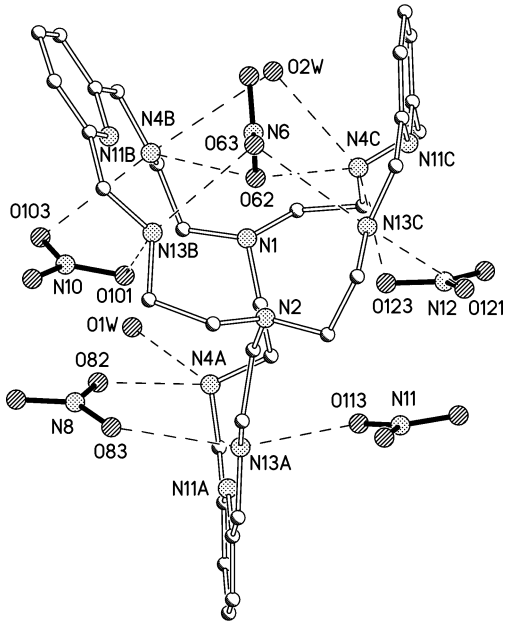

Fig. 14 Nitrate cryptate of R3P showing intercalation of one nitrate anion and stacking of two other pairs. Selected NH–ONO$_2$ distances: N4A–O82, 2.772(6); N13A–O83, 2.785(6); N13A–O113, 2.840(6); N13B–O101, 2.894(6); N13B–O63, 2.805(6); N13C–O63, 2.936(7); N13C–O121, 2.874(6) Å.

pairs of extracryptate anions, a nitrate–nitrate stacking motif similar to that observed within the cavity of R3Bm (Fig. 12). The facility of multiply bonded oxoanions or parts of oxoanions to participate in π-stacking with each other or with aromatic rings is an intriguing property, which we will have reason to revisit in later sections.

3 Tetrahedral dinegative oxoanions

Electrostatic interactions are accepted[12,31] as a major determinant of stability in anion complexation. Thus it was important to investigate the capacity for complexation of dinegative anions by our protonated cryptand hosts. The most useful initial comparison can be made using dinegative tetrahedral oxoanions where charge is the major or only differentiator from mononegative analogues. Structures were obtained[32] for selenate, chromate and thiosulfate cryptates of R3Bm. Of these the structure of the thiosulfate crypt (Fig. 15) is the most symmetric

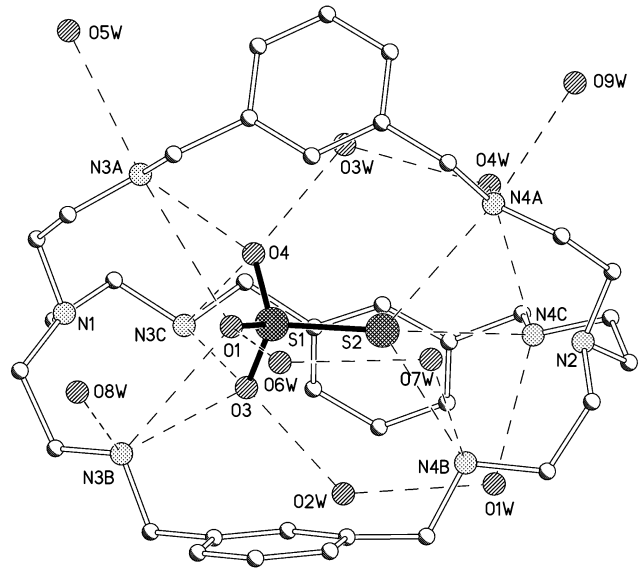

Fig. 15 Thiosulfate cryptate of R3BmH$_6^{6+}$. Selected NH–O and NH–S H-bond distances: N3A–O4, 2.861(4); N3A–O1, 3.214(5); N4A–S2, 3.455(3); N3B–O3, 2.957(4); N3B–O1, 3.059(4); N4B–S2, 3.298(3); N3C–O3, 2.852(4); N3C–O4, 3.087(4); N4C–S2, 3.491(3); O2W–O3, 2.781(4); O3W–O4, 2.712(4); O6W–O1, 2.681(4) Å.

and is free from disorder. The cation has approximate three-fold symmetry, and all four acceptor sites of the oxoanion are used to bind directly to the six protonated amines. The familiar 3-pronged crown motif whereby NH$^+$ functions are individually chelated (*via* bifurcated H-bonds) by a pair of adjacent oxoanion O-acceptors and in turn chelate each oxoanion O-acceptor, reappears here, together with some indirect water-mediated H-bonding, less direct and less important than in perchlorate, presumably because the second set of three NH$^+$ donors is occupied in bonding the thiosulfate sulfur. The anion is thus bound by six direct NH···O and three NH···S interactions (Table 2) which, together with the absence of disorder, suggests good fit between host and guest.

Table 2 H-bonds[32] between encapsulated anion, MO_4^{2-} and cryptand. M = Cr: **1**; M = Se: **2**; M = S(=S): **3**

	1	**2**	**3**
O1	2.766(8) N3b	2.820(6) N3a	3.059(4) N3b
	2.841(9) N3a	2.924(6) N3b	3.214(5) N3a
O2/S2	2.950(9) N4b	2.927(6) N4a	3.298(3) N4b
	3.214(10) N4a	3.116(6) N4b	3.455(3) N4a
			3.491(3) N4c
O3			2.852(4) N3c
			2.957(4) N3b
O4	2.75(3) N3c	2.653(12) N3c	2.861(4) N3a
	2.75(4) N3c′	2.913(13) N3c′	3.087(4) N3c

In the other dinegative oxoanion structures, the encapsulated anions are bound in slightly less symmetric fashion. In the chromate cryptate structure (Fig. 16) one of the protonated amines is not involved in intramolecular hydrogen bonding and

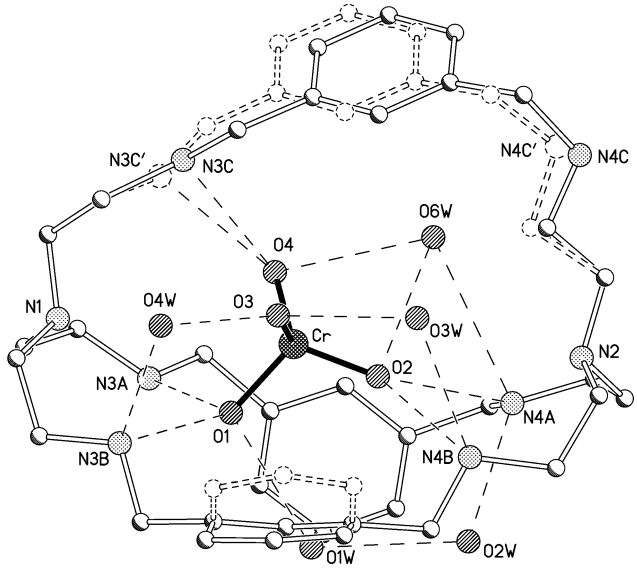

Fig. 16 Chromate cryptate of R3Bm H_6^{6+} showing direct and water mediated H-bonding and disorder in one strand. Selected H-bond distances: N3A–O1, 2.841(9); N4A–O2W, 2.734(9); N4A–O6W, 3.18(2); N3C–O4, 2.75(3); N3B–O1, 2.766(8); N3B–O4W, 2.912(13); N4B–O2, 2.950(9); N4B–O3W, 2.835(10) Å.

the section of the cryptand which contains this NH_2^+ is disordered. There are fewer direct intramolecular H-bond interactions than in the thiosulfate but they are overall shorter (Table 2). Lattice water and non-encapsulated oxoanion oxygens take up the remaining hydrogen bonding sites on both cryptand and encapsulated anion generating rings and chains running through the crystal lattice. The selenate structure (Fig. 17) also exhibits just five intramolecular N–H···O bonds tethering the included oxoanion to the protonated cryptand host; these are closely similar in average length to the set of H-bonds in the chromate structure.

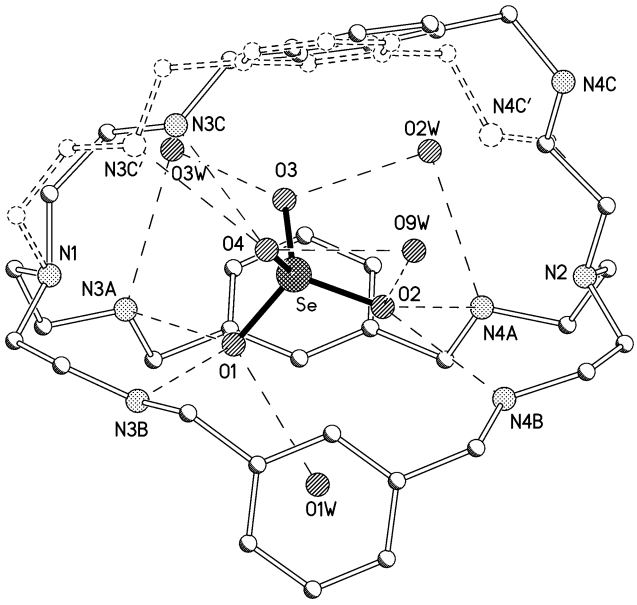

Fig. 17 Selenate cryptate of R3Bm H_6^{6+}. Selected H-bond distances N4A–O2, 2.927(6); N4A–O2W, 2.848(6); N3A–O1, 2.820(6); N3A–O3W, 2.884(6); N4B–O2, 3.116(6); N4B–O9W, 3.239(10); N3B–O1, 2.924(6); N3C–O4, 2.653(12)Å.

3.1 Quantitative solution measurements: dinegative oxoanions

Both ^{1}H NMR and pH-potentiometric methods of evaluating complexation constants were undertaken for this tetrahedral dinegative series of oxoanions. In constrast to the self-consistent log K_{app} values obtained by these different techniques for the mononegative oxoanions,[19,25,27] significant discrepancies arose between the values obtained using pH-metric and NMR methods for the dinegative anions. These differences can be attributed to the unsuitability of the NMR shift method for reliable determination of complexation constants greater than log $K \approx 4$.[20] Where complexation is strong, NMR shifts, given the inevitably large ratio of complexed: uncomplexed species, will be only slightly affected by change of stoichiometry and consequently complexation constants are not expected to be accurately determinable. Our best attempt at evaluation using this method resulted in approximate log K values of the order[19] of 4.9 for thiosulfate and selenate cryptates, which in comparison with the values for mononegative oxoanions (and those evaluated otherwise for dinegative oxoanions in Table 3) appear unconvincingly low.

pH-potentiometric methods are more appropriate to evaluation of complexation constants above log $K = 4$ and the values in (Table 3) are precise to within ± 0.02–0.06 at hexaprotonated, and ± 0.08–0.14 at diprotonated host level. Many of the values obtained by this method, particularly for the larger selenate and thiosulfate ions, are higher than any to date reported for complexation of tetrahedral dinegative oxoanions. It is noticeable that complexation constants at the tetraprotonated level of the host are still higher than log $K = 4$, and those at diprotonated level, where a charge-neutral complex eventuates, compare favourably with values for mononegative oxoanions complexed by hexaprotonated versions of these azacryptand hosts. This raises expectation of successful transport of dinegative oxoanions into nonpolar media followed by pH swing adjustment to release the oxoanion, as the basis of an extraction and recovery method for valuable or toxic dinegative oxoanions. The relatively high efficiency of the cleft-binding ligand R3P at the low protonation levels used for extraction is intriguing as well as potentially useful. In all cases the hexaprotonated forms of the cavity-binding ligands have the largest complexation constants, but this alters as the protonation level reduces, crossover to higher stability for the R3P complex occurring at pentaprotonated level for sulfate, and tetra- or tri- protonated level for the other two oxoanions. Presumably, greater conformational freedom in the cleft allows more energetically advantageous positioning of the guest in lower protonation states than is possible in the cavity-bound form. This is a consequence of the smaller number of NH^+ donors needed to bind any particular anion in the cleft conformation[25] together with a greater flexibility in response to repulsive interactions. The lower lipophilicity of R3P *versus* the other cryptands[25] will also influence, *via* entropic effects arising from desolvation processes, the magnitude of the observed complexation constants, but calorimetric data is currently lacking to confirm the size of this effect.

A recent study of sulfate complexation[20] over the pH range 2.5–11 evaluates log K for R3Bm hexaprotonated and heptaprotonated forms respectively, in 0.1 M NaOTs at 298.1 K, as 4.43(1) and 4.97(5), contrasting with the considerably higher values we obtain for dinegative systems, including sulfate (Table 3). In this paper the authors report difficulties with interpretation of complex stoichiometry from potentiometric data alone. Their observation of K dependency on anion concentrations suggest problems with correct model fitting. We were unable to recognise any heptaprotonated form of the R3Bm host, such as is considered responsible for sulfate complexation at the extreme acid limit of the pH range used by these authors. Nor is it realistic to suppose that monoprotonation of the sulfate ion is making an appreciable impact at pH values above 2.

However, the question of whether potentially protonable target dinegative anions are complexed in deprotonated dinegative or monoprotonated mononegative form, is one of im-

Table 3 Stepwise formation constants (log K_{app}/dm^3 mol^{-1}) for binding of dinegative oxoanions by R3Bm, R3F, and R3P as determined by pH-metry, I = 0.1 M OTs$^-$, T = 298 K

Species (L,H,X)[a]	R3Bm			R3F			R3P		
	SO_4^{2-}	SeO_4^{2-}	$S_2O_3^{2-}$	SO_4^{2-}	SO_4^{2-}	$S_2O_4^{2-}$	SO_4^{2-}	SeO_4^{2-}	$S_2O_4^{2-}$
1,6,1	6.57 ± 0.04	7.24 ± 0.05	8.51 ± 0.05	7.21 ± 0.03	7.27 ± 0.06	7.65 ± 0.07	6.08 ± 0.03	5.38 ± 0.06	6.00 ± 0.06
1,5,1	4.72 ± 0.07	5.39 ± 0.04	6.40 ± 0.09	5.21 ± 0.06	5.38 ± 0.08	5.11 ± 0.10	5.55 ± 0.03	4.93 ± 0.06	5.63 ± 0.05
1,4,1	3.70 ± 0.12	4.77 ± 0.06	5.49 ± 0.08	4.32 ± 0.06	4.53 ± 0.08	5.09 ± 0.08	5.19 ± 0.03	4.66 ± 0.08	5.30 ± 0.06
1,3,1	3.47 ± 0.05	4.18 ± 0.04	4.74 ± 0.05	4.02 ± 0.03	4.15 ± 0.06	4.56 ± 0.07	4.84 ± 0.02	4.34 ± 0.06	4.95 ± 0.05
1,2,1	3.06 ± 0.10	3.64 ± 0.08	4.12 ± 0.10	3.37 ± 0.06	3.52 ± 0.08	3.83 ± 0.14	4.12 ± 0.04	3.87 ± 0.07	4.25 ± 0.06

[a] In all cases the oxoanion is assumed to be doubly deprotonated; measurements over the pH range 3–11.

Table 4 Stepwise formation constants (log K_{app}/dm^3 mol^{-1}) for complexation of carboxylate anions by R3Bm, R3F, and R3P as determined by pH-metry (I = 0.1M OTs, T = 298 K)

	X = acetate			X = lactate			X = oxalate			X = malonate		
Species (L,H,X)[a]	R3Bm	R3F	R3P	R3Bm	R3F	R3P	R3Bm	R3F	R3P	R3Bm	R3F	R3P
(1,7,1)							13.83 ± 0.06	7.17 ± 0.10	7.61 ± 0.10	5.77 ± 0.13	5.64 ± 0.17	8.07 ± 0.08
(1,6,1)	4.00 ± 0.04	3.73 ± 0.09	5.01 ± 0.06	3.86 ± 0.06	3.50 ± 0.06	5.14 ± 0.10	10.71 ± 0.06	8.30 ± 0.05	8.23 ± 0.06	7.22 ± 0.08	6.62 ± 0. 10	8.34 ± 0.10
(1,5,1)	4.21 ± 0.04	3.99 ± 0.04	5.73 ± 0.04	4.06 ± 0.05	3.75 ± 0.04	5.53 ± 0.08	8.64 ± 0.08	7.12 ± 0.04	7.34 ± 0.08	6.20 ± 0.08	5.55 ± 0.0 8	7.78 ± 0.08
(1,4,1)	4.27 ± 0.04	4.01 ± 0.05	5.65 ± 0.06	3.61 ± 0.08	3.30 ± 0.06	5.14 ± 0.09	7.15 ± 0.05	5.53 ± 0.06	6.64 ± 0.08	5.79 ± 0.06	5.00 ± 0.0 9	7.21 ± 0.08
(1,3,1)	4.05 ± 0.04	3.93 ± 0.04	5.34 ± 0.04	3.45 ± 0.07	3.13 ± 0.06	4.87 ± 0.07	5.49 ± 0.07	4.82 ± 0.04	5.92 ± 0.07	4.87 ± 0.06	4.42 ± 0.0 8	6.32 ± 0.06
(1,2,1)	3.67 ± 0.07	3.43 ± 0.08	4.47 ± 0.06	3.12 ± 0.10	2.91 ± 0.08	3.94 ± 0.15	—	4.05 ± 0.07	4.66 ± 0.10	—	3.62 ± 0.12	5.16 ± 0.08

[a] Except for the 1,7,1 species, the calculation of the constants assumed the anion to be deprotonated (see discussion in text).

portance in many of these oxoanion systems. It can be probed for the chromate system because the target anions have, in this case, the advantage of being coloured and are thus capable of spectroscopic monitoring. Although at the pH at which the anion cryptate was synthesised, the protonation equilibrium strongly favours hydrogen chromate, electronic absorption spectroscopy clearly indicates (Fig. 18) complexation of the

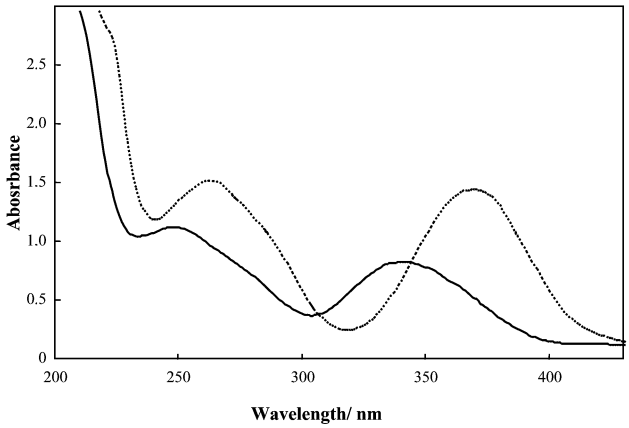

Fig. 18 UV spectra for K_2CrO_4 in the absence (—) and presence (. . . .) of R3Bm at pH 4.6. $[K_2CrO_4]$ = [R3Bm] = 0.6 mM.

anion in its chromate form. The relative order of the second deprotonation constant in this series of tetrahedral dinegative oxoanions (pK_as: chromic, 6.49; sulfuric 1.50; selenate 1.80, thiosulfate 1.72) indicates that here chromate is the only ion that could be protonated at pH ≈ 3. On this basis it appears that the electrostatic driving force for complexation favours the dinegatively charged guest in all four cases.

4 Carboxylate anions

The carboxylate series represents a different but not less important class of oxoanions. Small di- and tricarboxylates are crucial constituents of many essential metabolic processes,[5,33] including the citric acid and glyoxylate cycles. Because of the importance of such systems, a significant amount of work has been carried out with polyammonium macrocyclic receptors such as O-bisdien and polyazacycloalkanes[13,15] capable of polyprotonation in the neutral pH region. Oxalate and malonate are among the dicarboxylates whose complexation is quantitatively studied in this earlier work (see Table 1).

With our protonated cryptand hosts, the carboxylates acetate, lactate, malonate and oxalate were studied, the last in some detail (Table 4). With the first three, potentiometric analysis is complicated by the fact that the guest anion is capable of protonation in the pH-range required for examination of the host protonation equilibria. For malonate for example, it is thus impossible, on the basis of potentiometry alone, to unambiguously assign the 1,7,1, species to complexation of the mononegative (monoprotonated) anion by the hexaprotonated azacryptand or complexation of dinegative anion by heptaprotonated azacryptand, or indeed to some combination of both. The acid and base dissociation constants of the constituents give some guidance in this respect; thus pK_as for oxalic (1.25, 4.29) acetic, (4.76) and malonic (2.85, 5.69) acids show that the order of basicity for the monoprotonated carboxylate function is malonate > acetate > oxalate. Thus, the existence of monoprotonated malonate is a real possibility at moderately acid pH while monoprotonated oxalate is the least likely of the three. It must also be remembered that we have, in the chromate system, independent evidence showing that charge selectivity in this cryptand series can act to disturb the guest protonation equilibrium in favour of the dinegative anion.

There does not seem to have been any previous quantitative study of the complexation of the monocarboxylate, acetate, with polyammonium-type ligands, whether cryptate or macrocyclic (although it has been shown to be moderately strongly complexed by specially designed podate or calixarene H-bonding hosts[34,35]). However our studies reveal relatively large formation constants for complexes of acetate with cryptand hosts (Table 4). These are larger than for the tetrahedral or trigonal inorganic monoanions,[19,25,27] because of the greater charge density which attends oxygen deprotonation in a carboxylate. However at the low pH which favours the neutral acetic acid species, the anion cryptate formation constants are lower than those at higher pHs associated with binding of acetate by penta-, tetra- or triprotonated hosts. The R3P system is particularly interesting as the binding constants shown in that case are anomalously high, suggesting the existence of additional, *e.g.* stacking or strong H-bonding, interactions: similar perhaps to those seen in oxalate analogues (*qv*). We lack structural data, however, to confirm such speculation.

In keeping with its higher acidity, the lactate anion shows its strongest complexation at relatively higher *i.e.* pentaprotonated host levels; once again the pH at which the hexaprotonated host dominates is low enough to permit significant formation of the weakly complexed neutral carboxylic acid form of the guest. Once again the R3P host binds the monocarboxylate appreciably more strongly than the other cryptands.

Within our cryptand systems, the malonate ion, which is capable of acting as a dicarboxylate under near neutral conditions, shows binding constants (Table 4), in the same range as those of dinegative tetrahedal oxoanions, but with the effect of easier guest protonation superposed. The highest formation constants are seen at $[H_6LA]^{4+}$ host levels. At lower pH (< 4), the presence of a sizeable proportion of the mononegative hydrogen malonate in the equilibrium mixture reduces the value of the log *K* observed for 1,7,1 complexation. However at the more basic pH associated with protonation levels at or below 5, the dinegative malonate ion is expected to dominate. Once again the pyridino-linked host, R3P, shows anomalously high complexation constants: even at acidic pHs where the monoprotonated mononegatively charged anion would normally be expected to dominate, log *K*s are significantly higher than those obtained for acetate, suggesting disturbance of the anion protonation equilibrium to accord with charge selectivity preferences. Comparison with the cavity-binding hosts R3Bm and R3F indicates that such disturbance if indeed present with these ligands, is less effective. This may perhaps derive from more efficient encapsulation of the relatively large dicarboxylate in the cleft-binding R3P host. The species distribution diagrams (see ESI† for malonate with R3Bm and R3P hosts) illustrates the difference between this pair of systems; the dominance of the neutral LH_2A species in the R3P system above pH 9 is promising for extraction applications as is the relatively high value of its formation constant (Table 4).

In other examples of coordination of malonate,[12,15,17] using O-bistren and O-bisdien hosts, weak binding of this oxoanion was noted (Table 1): log *K*s in the range 2–4 irrespective of whether the host is macrocyclic or cryptate). This was attributed partly to poor steric match, partly to the effects of protonation of the guest.

Oxalic acid, on the other hand, exhibits dissociation constants which largely remove it from competition with the cryptand ligand for protons. A further advantage is that it can easily be accommodated within the cavity of the azacryptand. Even so, we were surprised by the size of the complexation constants obtained upon pH-potentiometric analysis (Table 4), particularly in the case of R3Bm. These include the largest binding constants to our knowledge so far established[36] for complexation of any dinegative anion within a cryptand. Table 4 shows that formation of a 1,7,1 species is especially favourable in the

case of the R3Bm host while in other cases the formation constant for such species is lower than for the 1,6,1 analogue. It appears that the strong complexation of oxalate by this host reduces the host acidity so much that an additional protonation is permitted although it is impossible to decide on the basis of potentiometry alone the extent to which 1,7,1 species represents complexation of nonprotonated anion by heptaprotonated host *versus* monoprotonated anion by hexaprotonated host. For the more acidic R3F and R3P cryptand hosts the possibility of heptaprotonation is less likely and the lower complexation constants evaluated at 1,7,1 level are consistent with a sizeable proportion of the mononegative anionic guest. However, the region in which the 1,7,1 species exists extends to pH values where Ox^{2-} is normally expected to be protonated, so the formulation is likely to represent some combination of both processes in all three cases.

The observation of anomalously large oxalate complexation constants enhances the importance of structural characterisation, so crystallographic data were obtained for all three anion cryptates. Figs. 19 and 20 show the structures of the inclusive oxalate cryptates of $R3BmH_6^{6+}$ and $R3FH_6^{6+}$. Some

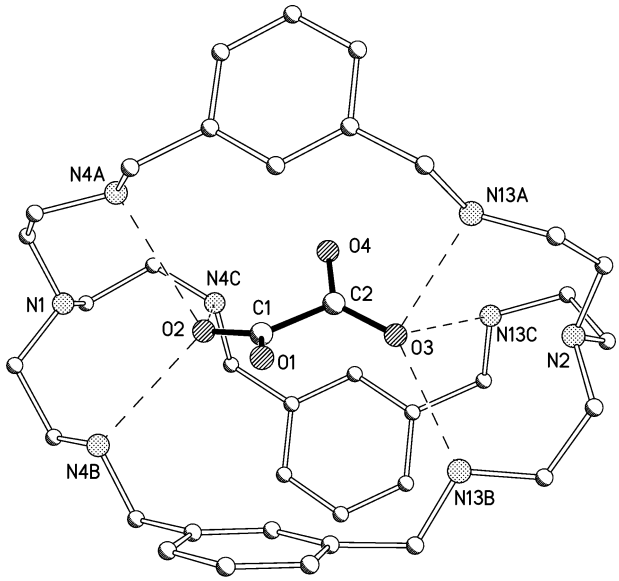

Fig. 19 Oxalate cryptate of $R3BmH_6^{6+}$ showing direct NH^+–$O_{oxalate}$ H-bonds. Selected H-bond distances: N4A–O2, 2.931(7); N4B–O2, 2.763(7); N4C–O2, 2.817(8); N13A–O3, 3.038(7); N13B–O3, 2.831(7); N13C–O3, 2.819(7) Å. Shortest C=O to π-ring distance 3.172 Å.

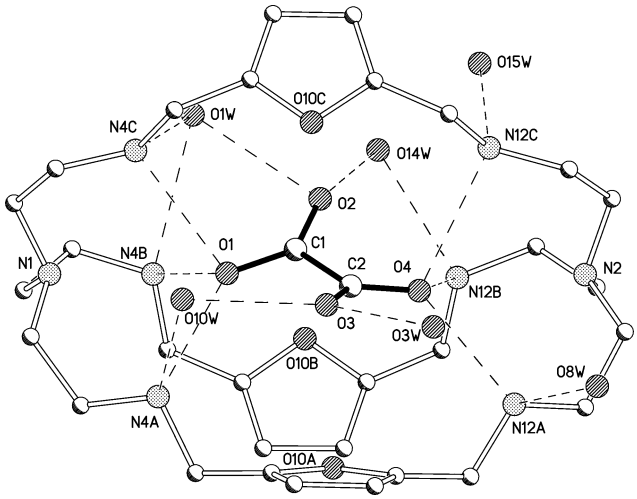

Fig. 20 Oxalate cryptate of $R3FH_6^{6+}$ showing direct and indirect H-bonding. Selected NH–$O_{oxalate}$ distances: N4A–O1, 2.762(7); N4B–O1, 2.846(7); N4C–O1, 2.912(7); N12A–O4, 2.740(7); N12B–O4, 2.936(7); N12C–O4, 2.834(7) Å. Shortest C=O to π-ring distance 3.052 Å.

unusual aspects are immediately apparent; the first surprise being the twisting of the oxalate from its normal planar conformation. In the oxalate-host assembly, one O from each carboxylate end of the guest is involved in direct NH···O hydrogen-bonding, where it makes a 4-centred H-bond to the set of three NH^+ donors from the appropriate end of the host. This leads to polarisation of the carboxylate function; the oxygen involved in this direct hydrogen-bonding binds carbon with a relatively long bond (C–O bond length 1.27, 1.28 Å respectively) while the remaining oxygen binds carbon with a significantly shorter bond length (1.23,1.24 Å approx.). On inspection of the structure it can be seen that the shorter carbonyl bond lies close to and parallel with one or more of the aromatic rings of the cryptand linker. There are C=O to aromatic distances below 3.6 Å, suggesting the existence of π–π stacking interaction between carbonyl-type carboxylate and aromatic rings. This interaction appears to be the one that drives the twisting of oxalate from its normal planar conformation[36] (admittedly not a very demanding alteration in energy terms). Such distortion in response to host geometry is a persuasive example of the contribution of inorganic/organic π-stacking interactions to the energetics of anion complexation.

The oxalate cryptate formed with R3P[19] adopts a quite different conformation. Here (Fig. 21) the host again operates in

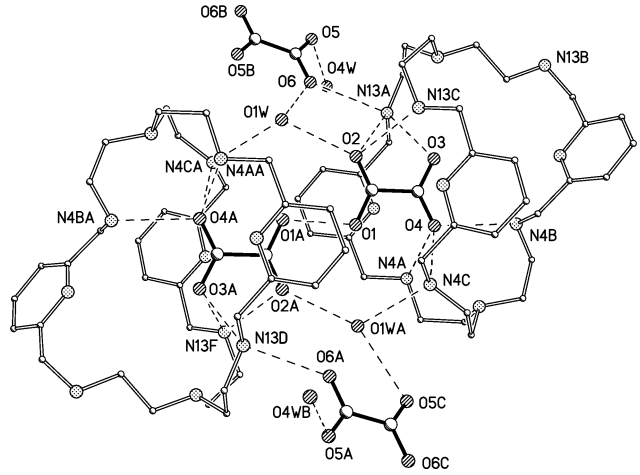

Fig. 21 Oxalate cryptate of $R3PH_6^{6+}$ showing H-bond dimer linked by strong H-bond O1–O1A, 2.474 Å. Selected NH–$O_{oxalate}$ H-bond distances: N4A–O4, 2.852(6); N4B–O4, 2.785(6); N4C–O4, 2.751(6); N13–O3, 2.895(6) Å.

cleft- rather than cavity-binding mode, but the oxalate guest slots as far as possible into a relatively shallow groove, leaving one end protruding into the aqueous environment. This end, being subject to the conditions ambient in water, can become protonated under the low pH conditions used for synthesis, and the protonated end acts as a H-bond donor. Between the pair of protruding oxalate guests a short, possibly symmetric, oxalate/semioxalate hydrogen bond exists, which brings the pair of cryptates together into a dimer.

The consequence of this set of unusual and effective interactions explains the exceptionally high binding constants for these protonated azacryptand oxalates. The binding constants indeed are so high as to suggest effective competition[19] with cations such as Fe^{II} or Ca^{II} for oxalate and to make it possible to conceive of detoxification applications for the systems, should the cryptands themselves prove to have satisfactorily low toxicity.

5 Phosphate systems

The previous discussion illustrates the difficulties which attend interpretation of results of complexation of these protonated cryptand hosts with the anions of dibasic acids. These problems

are exacerbated where tribasic acids are involved. Preliminary attempts were made to measure the solution complexation of phosphate species by these cryptand hosts, but the results obtained have been analysed only to the stage of obtaining overall complexation constants with no attempt to assign stepwise constants (see Table in ESI†). Measurements made over a range of pHs report on the equilibria of the three differently charged/protonated forms of the anions which coexist in aqueous solution while fixed pH ^{31}P NMR studies suggest that the protonation equilibria of the guest are disturbed in presence of the cryptand host, as was shown spectroscopically for the chromate system. Added to this the sizeable complexation shifts expected for these moderately strongly hydrogen-bonded species, and the assignment of time-averaged NMR shifts to the effects of complexation equilibria becomes a non-trivial exercise. However analysis of pH-metric and NMR results for phosphate systems is certainly worth the necessary investment of effort, and future work on these systems is planned.

6 Protonated cryptand oxoanion hosts; general structural considerations

For the tren-derived azacryptands, the general pattern is to protonate all six secondary amines but not the tertiary bridgeheads. Consequently, each $RR'NH_2^+$ unit can act as donor for two hydrogen bonds so that the protonated cryptand can form twelve hydrogen bonds (or more if bifurcated bonds are present); in most cases this is the observed pattern. Geometric considerations mean that no more than six of the N–H bonds can be oriented convergently towards an anionic guest in the cavity, the others diverge and lead to extensive hydrogen-bonded networks running through the lattice, typically involving the cryptate, unencapsulated anions and water molecules. Examples involving six direct NH···O hydrogen bonds from the protonated amine to the encapsulated guest(s) are relatively uncommon (Figs. 12, 15 and 20) and this pattern appears to indicate a good fit. Where the fit is less good the hydrogen bond capacity of anion and cryptand can be better satisfied by "indirect" NH···OH···O links in which the protonated amine is hydrogen-bonded to a water molecule which is, in turn, hydrogen-bonded to the encapsulated anion (see, for example, Figs. 7, 16 and 17). In other examples, one oxygen atom of the bound oxoanion is not involved in any hydrogen-bonding (*e.g.* O2 in Fig. 10, O11 in Fig. 7).

An alternative mode of anion coordination is the cleft-bound arrangement; no single oxoanion is bound in the centre of the cavity but rather one or more ions are bound in each of the three clefts between adjacent strands of the cryptate. In this configuration both protons on the amines can be directed into clefts. An example with approximate three-fold symmetry is $[(H_6R3Bp)(Tos)_6]$ (Fig. 4), while Fig. 8 shows a less symmetric example. The extensive hydrogen-bonding in the tosylate structure underlines the observation that, although it is prevented from binding inside the cryptand cavity, it is not an "innocent" anion in these systems – though it is a convenient calibration standard for solution studies.

The neutral R3P cleft or "clip" conformation, Fig. 9, shows a π–π interaction between two of the pyridine rings (responsible for the clip) but it is also notable that all six NH groups in this structure make divergently directed hydrogen bonds to solvate molecules in the lattice. Some H-bonding is usually observed in structures of neutral crypts[29,19] but electrostatic considerations mean it is weaker than in protonated systems.

Two complexes involving the octaprotonated form of the R3P ligand have been structurally characterised. At first glance it is surprising in the perchlorate complex,[23] (Fig. 8) that only two of the three pyridine groups should be protonated, however, examination of the lattice shows that both protonated pyridine groups are involved in hydrogen-bonding while the non-protonated ring is not. Presumably protonation of the pyridine is stabilised by hydrogen-bonding in the solid state. The apparent reluctance of this cryptand to bind anions in the central cavity may be connected with a preference for using one or more pyridines as donor or acceptor in H-bonding.

Overall the crystal structures are controlled by the requirement to minimise the energy of the lattice which will involve maximising the total hydrogen-bonding. In solution however solvation effects must be considered. Because we have not yet completed our calorimetric study of these systems[37] we may have failed to resist the temptation to overestimate the importance of enthalpic contributions to the measured equilibrium constants. Careful studies on analogous azamacrocyclic systems[12] have shown that in many cases, where the guest is not protonated, anion complexation is near thermoneutral, with important entropic contributions deriving from desolvation of both host and guest. In particular, it is possible that log *K* differences between similarly charged oxoanions may have their origin in desolvation phenomena.[38]

7 Cascade complexation of oxoanions

An early objective of the Lehn cryptand strategy[39] was the achievement of cascade complexation, whereby substrates coordinated by dinuclear cations coordinated within a cryptand would, while activated by reason of their coordination and under the steric protection of the host, undergo catalytic chemistry of the kind achievable by enzymes. The first stage of this objective: bridging coordination of anions within dinuclear cation cryptates, is readily attainable, at least within azacryptands where less than six donors are provided by the host. There are many sets of such ternary complexes, often dubbed "cascade complexes", which can be perceived as deriving from complexation of a dicoordinating anion by the dinuclear cryptate host. Many of these involve nitrogen donors,[18,40,41] but some cryptate hosts tether oxoanions, and it is mainly these systems which we will discuss in this section. The general field of ion cascade chemistry has been recently reviewed,[40] so we will restrict this brief account to selected results not included in that review.

Our cryptand hosts are well preorganised for complexation and their dinuclear transition ion complexes in general exhibit high formation constants.[18] However as the comparatively smaller values for Ni(II) indicate, the number of intrinsic donors furnished by the azacryptand hosts to each coordination site often falls short of that ideally preferred by many transition ions. These ions thus readily accept extra donors from anions of the appropriate length to slot into the cryptate cavity. Our earliest observation of such behaviour arose from the attempt to synthesise a dicopper(II) cryptate of the furano-linked cryptand R3F which resulted in the isolation of a μ-hydroxo dicopper(II) cation.[18] The bright green crystalline compound isolated from a similarly coloured solution was structurally characterised (Fig. 22) and shown to contain a collinear Cu–O(H)–Cu assembly which, despite the ≈ 3.9 Å separation of the paramagnets, is strongly interacting and virtually diamagnetic. However no analogous μ-hydroxo dicopper(II) cryptate could be isolated from the superficially similar host R3Bm; the products obtained from that system under aerobic conditions were eventually shown[42] to contain bridging 1,3 carbonato- (or related) ions (see Fig. 28). This was the earliest indication of a steric distinction between the 2,5-furano- and *m*-xylyl- linked hosts, a distinction which has since been well-documented in our own work and that of others.[41,42] Triatomic N- or O- donor anionic bridges, on the other hand, are easily accommodated within the apparently more spacious *m*-xylyl linked cryptate host.

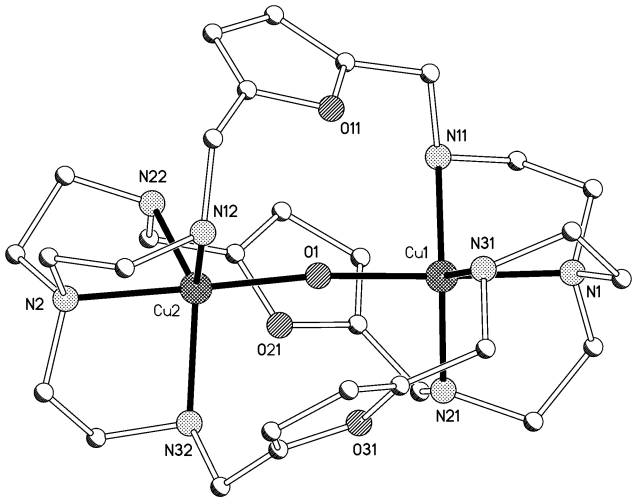

Fig. 22 $[(Cu_2OH)R3F]^{3+}$ cation selected distances and angles: Cu1–O1, 1.957(4); Cu1–N1, 2.075(5); Cu1–N31, 2.129(5); Cu1–N21, 2.144(5); Cu1–N11, 2.173(5); Cu2–O1, 1.948(4); Cu2–N2, 2.074(5); Cu2–N32, 2.130(5); Cu2–N22, 2.149(5); Cu2–N12, 2.182(6) Å; Cu(2)–O(1)–Cu(1), 174.0(3)°.

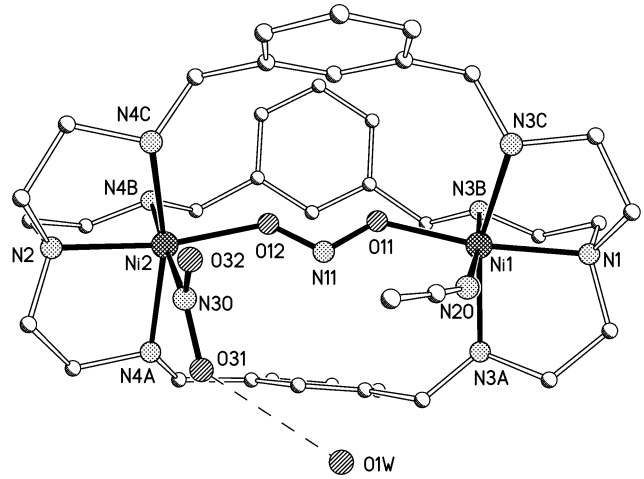

Fig. 23 $[Ni_2(NO_2)_2R3Bm.MeCN]^{23+}$ cation showing the previously unreported 1,3 O,O mode of nitrite bridging. Selected distances and angles: Ni1–O11, 1.989(3); Ni1–N1, 2.101(4); Ni1–N3B, 2.138(4); Ni1–N3A, 2.145(4); Ni1–N20, 2.166(4); Ni1–N3C, 2.168(4); Ni2–O12, 2.006(3); Ni2–N2, 2.074(4); Ni2–N4C, 2.143(4); Ni2–N4B, 2.148(4); Ni2–N30, 2.173(5); Ni2–N4A, 2.207(4); O11–N11, 1.264(5); N11–O12, 1.253(5) Å, N11–O11–Ni1, 130.0(3), O12–N11–O11, 112.0(4), N11–O12–Ni2, 131.6(3)°.

7.1 Nitrito bridges

As already established for dicoordinating N-donor anions, unfamiliar modes of bridging can be enforced within the unusual geometry of the cryptand cavity. The previously unknown 1,3 *trans* O,O bridging mode of nitrite has been structurally characterised (Fig. 23) within a dinickel R3Bm cryptate.[43] The Ni–O average distances are ≈ 2.00 Å, showing good fit for the bridging anion within the cavity, and this new mode of bridging is associated with moderate antiferromagnetic interaction (Table 5). A second NO_2^- is coordinated *via* the nitrite N, as nitro-, to the Ni(2) centre, showing that nitro-coordination is still favoured for Ni(II) within this host, and that the unusual choice of O,O nitrito- bridging derives from the good steric compatibility offered by the triatomic link. Together with infrared spectroscopic criteria, the magnitude of the antiferromagnetic coupling in related systems indicates that the O,O nitrito bridging mode is present in structurally uncharacterised diCu(II) and diCo(II) analogues (Table 5).

The X-ray structure of a dinickel nitrito complex of the effectively smaller-cavity host R3F (Fig. 24) does not, however, involve bridging oxoanion; in this case two cryptand strands are linked by a pair of moderately short NH—O_{furan} H-bonds making a flat basket shape for the host within which the two nitrites separately chelate each Ni(II) cation, completing the desired hexacoordination. The weak magnetic interaction observed is consistent with the absence of a bridging pathway.

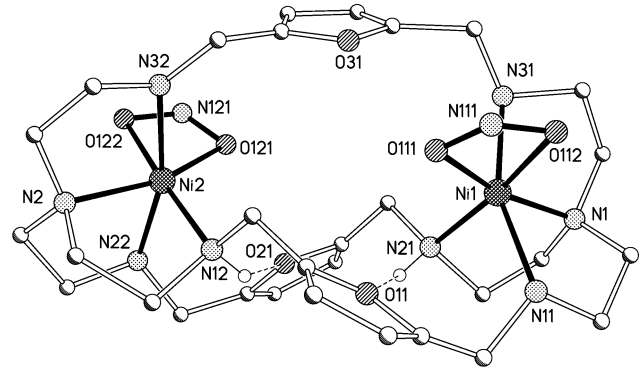

Fig. 24 $[Ni_2(NO_2)_2R3F]^{2+}$ cation showing cavity partitioned by strand-linking H-bonds. Selected bond distances and angles: Ni1–N1, 2.09(2); Ni1–O111, 2.09(2); Ni1–N31, 2.10(2); Ni1–N21, 2.13(2); Ni1–N11, 2.16(2); Ni1–O112, 2.223(18); Ni2–N2, 2.08(2); Ni2–O121, 2.08(2); Ni2–N12, 2.11(2); Ni2–N32, 2.12(2); Ni2–N22, 2.13(2); Ni2–O122, 2.16(2); N12– O21, 2.95(2), N21–O11, 3.02(2) Å.

7.2 Carbonato bridges

Another interesting case study illustrating the relative ease of accommodation of oxoanions in dinuclear cryptate hosts is provided[42] by the carbonato system. This coordinatively adaptable system has the option of using various bridging modes: single-atom or triatomic, together with some inter-

Table 5 Magnetic data for dicopper(II), dinickel(II), and dicobalt(II) cryptates with $(CO_3)^{2-}$, $(MeCO_3)^-$ and $(NO_2)^-$ bridges

Complex	Coordination mode	μ_{275}/μ_B	μ_{80}/μ_B	$-2J/cm^{-1}$	g
$[Cu_2L^1(CO_3)](ClO_4)_2.2H_2O^a$	*anti-anti* μ-η_1,η_1	1.50	0.81	210 ± 5	1.93 ± 0.01
$[Ni_2L^1(CO_3)](ClO_4)_2.2H_2O.2MeOH$	*anti-anti* μ-η_1,η_1	2.82	2.56	1.9 ± 0.2	2.10 ± 0.01
$[Co_2L^1(CO_3)](ClO_4)_2.2H_2O$	μ-η_1,η_2	4.48	4.18	2.8 ± 0.1	2.27 ± 0.01
	anti-anti μ-η_1,η_1			11 ± 1	2.40 ± 0.01
$[Ni_2L^2(CO_3)](ClO_4)_2^a$	μ-η_2,η_2	2.41	1.26	108 ± 1	1.97 ± 0.01
$[Cu_2L^1(MeCO_3)](ClO_4)_3].4H_2O$	*syn-anti* μ-η_1,η_1	1.90	1.84	11 ± 1	2.17 ± 0.01
$[Ni_2L^1(MeCO_3)](ClO_4)_3.4H_2O$	*syn-anti* μ-η_1,η_1	3.09	2.84	10.1 ± 0.1	2.15 ± 0.01
$[Co_2L^1(MeCO_3)](ClO_4)_3.4H_2O$	*syn-anti* μ-η_1,η_1	4.39	4.27	1.4 ± 0.1	2.19 ± 0.01
$[Cu_2L^1(NO_2)_2](ClO_4)_2.3H_2O^b$	*anti-anti* μ-η_1,η_1	1.70	1.07	127 ± 1	2.12 ± 0.02
$[Ni_2L^1(NO_2)](ClO_4)_3.MeCN^a$	*anti-anti* μ-η_1,η_1	2.98	2.66	18.5 ± 0.1	2.12 ± 0.01
$[Co_2L^1(NO_2)](ClO_4)_3.3H_2O^c$	*anti-anti* μ-η_1,η_1	4.89	4.34	7.0 ± 0.4	2.46 ± 0.01
$[Ni_2L^2(NO_2)_2]_2(ClO_4)_2.7H_2O^b$	non-bridging η_2,η_2	3.34	3.28	3.4 ± 0.4	2.36 ± 0.01

L^1 = R3Bm L^2 = R3F [a] Fit requires a paramagnetic impurity term evaluated as (6%), (1.8%) and (7%) respectively. [b] Parameters derived from data in the range 70–280 K. [c] Fit requires an interdimer exchange which is small (3 K) but ferromagnetic.

mediate combinations of both, according to the space available in the host assembly.

With the effectively smaller hosts derived from R3F, the product of treatment of dinuclear cryptates of Ni(II) or Co(II) with preformed carbonate anion *in situ* is the *bis*-chelating $\eta_2\eta_2$ -bridged mode complex (Fig. 25). The M–O–M distances at

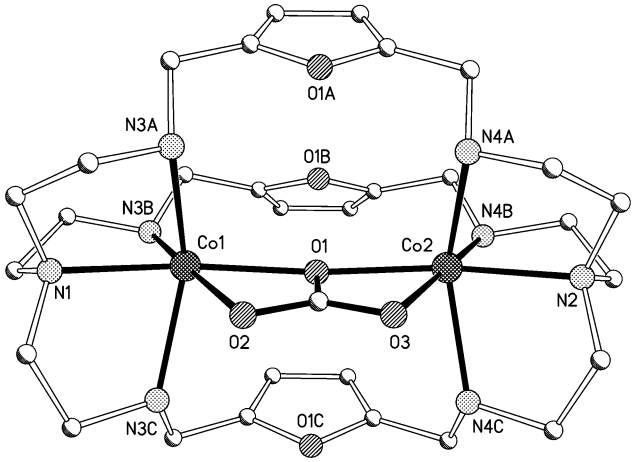

Fig. 25 $\eta_2\eta_2$ mode of bischelating carbonato-bridging within R3F; selected distances and angles: Co1–O2, 2.146(9); Co1–O1, 2.151(9); Co1–N3B, 2.165(12); Co1–N1, 2.180(11); Co1–N3A, 2.236(10); Co1–N3C, 2.261(11); Co1–Co2, 4.292(3); Co2–O1, 2.145(9); Co2–N4B, 2.154(12); Co2–O3, 2.157(9); Co2–N2, 2.177(10); Co2–N4A, 2.205(10); Co2–N4C, 2.247(10) Å; Co2–O1–Co1, 175.1(4)°.

2.146 Å each show that this is close to an effective single-atom-bridge, generating a metal–metal distance just short of 4.3 Å; the magnetic interaction mediated by the bridge provides confirmation of the effectively monatomic pathway, *via* relatively strong antiferromagnetic coupling constants of $2J = -108$ cm^{-1} for the nickel(II) and -30 cm^{-1} for the cobalt(II) cryptates, in line with coupling constants obtained for other structurally characterised $\eta_2\eta_2$-bridged carbonate complexes.[42]

Within the *m*-xylyl spaced cryptates, however, addition of the preformed carbonato-ligand generates the 1,3 O,O-bridged product either in the *anti-anti* bridged mode (Fig. 26) as in the

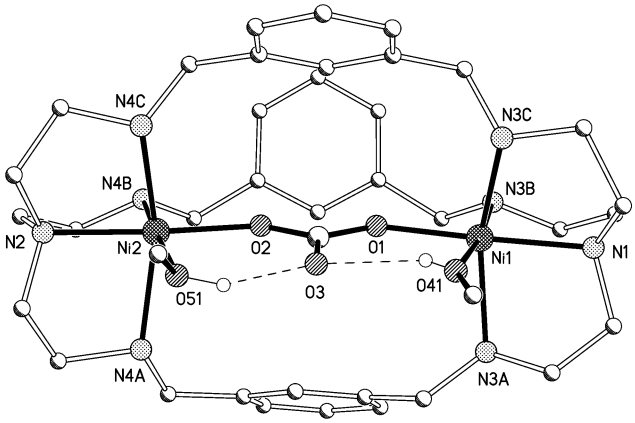

Fig. 26 *Anti-anti* 1,3-bridging mode of carbonato within $[NiCu_2R3Bm(MeOH)_2]^{4+}$ host. Selected distances: Ni1–O1, 1.946(7); Ni1–N1, 2.106(10); Ni1–N3A, 2.151(8); Ni1–N3C, 2.126(8); Ni1–N3B, 2.126(8); Ni1–O41, 2.445(8); Ni2–O2, 1.969(7); Ni2–N2, 2.081(11); Ni2–N4C, 2.124(9); Ni2–N4B, 2.136(9); Ni2–O51, 2.202(8); Ni2–N4A, 2.243(10); Ni1–Ni2, 6.0178(19); O41–O3, 2.552(12); O51–O3, 2.513(11) Å.

dicopper(II), dinickel(II) or dicobalt(II) (complexes or in the *syn-anti* mode as in dizinc(II) (Fig. 27). As expected, these 1,3-bridging assemblies are only moderately effective in mediating antiferromagnetic interaction (Table 5).

An interesting catalytic reaction takes place when dinuclear cryptates of R3Bm are allowed to crystallise in methanol solution under aerobic conditions without the addition of

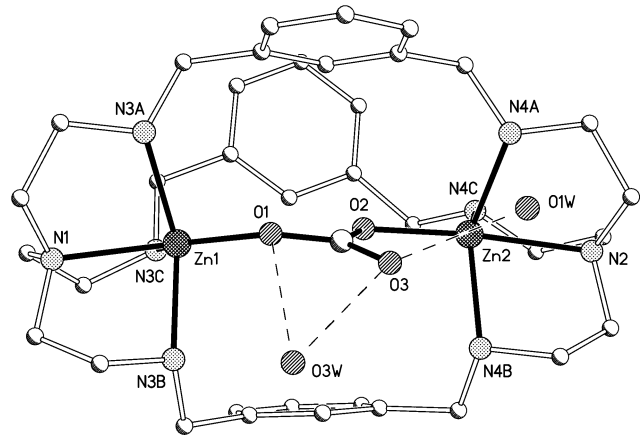

Fig. 27 *Syn-anti* bridging mode of carbonato within $[Zn_2R3Bm]^{4+}$ host. Selected distances: Zn1–O1, 1.989(2); Zn1–N3C, 2.095(3); Zn1–N3A, 2.177(3); Zn1–N3B, 2.188(3); Zn1–N1, 2.232(3); Zn2–O2, 1.979(2); Zn2–N4C, 2.100(3); Zn2–N4A, 2.137(3); Zn2–N4B, 2.159(3); Zn2–N2, 2.269(3); Zn1–Zn2, 5.3308(6); O1W–O3, 2.697(3); O3W–O3, 2.812(4); O3W–O1, 3.098(4) Å.

preformed carbonate ion. In the case of dicobalt(II), dinickel(II) dicopper(II) and dizinc(II) cryptates the product of this reaction is the methylcarbonato bridged cryptate (Fig. 28). While the

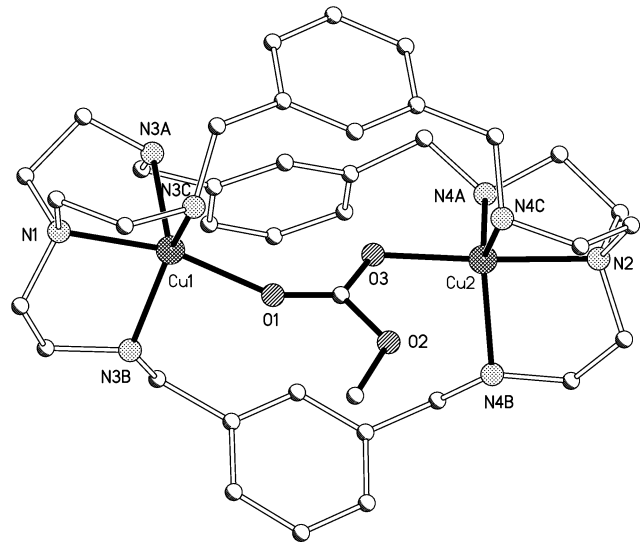

Fig. 28 Methylcarbonato-bridged dicopper(II) assembly formed spontaneously in methanol solution by CO_2 absorption. Selected distances: Cu1–O1, 1.963(3); Cu1–N1, 2.040(3); Cu1–N3C, 2.061(3); Cu1–N3B, 2.074(3); Cu1–N3A, 2.232(3); Cu2–O3, 1.941(3); Cu2–N2, 2.034(3); Cu2–N4C, 2.086(3); Cu2–N4A, 2.130(3); Cu2–N4B, 2.158(3); Cu1–Cu2, 5.6554(6) Å.

mechanism of this reaction has yet to be established, it appears that insertion of CO_2 into coordinated methoxo has taken place, generating the monomethyl ester: an illustration of the cascade reactivity envisaged in Lehns original strategy.

This reaction does not take place within the R3F host, nor so far as we can ascertain, elsewhere, except[44] within the steric protection of a cavity-shaped binucleating host. It seems likely, then, that the spacing of the pair of transition ions is crucial to success of the catalysis. The reluctance of R3Bm to accommodate a single atom bridge is likely to be an important factor; allowing the proximate coordination of reagents within the steric protection of the cage, while preventing access to the thermodynamic sink of the single-atom bridged product, be it hydroxo or carbonato.

7.3 Shape selectivity in cascade cryptate hosts

The design of cage ligands with suitably spaced coordination sites is of some interest in connection with this type of cascade

reactivity. Subtle factors come into play in generating the effectively smaller cavity size noted for R3F *vs* R3Bm, given that both are 5-atom bridges.

The head group (phenyl, pyridine or furan) restricts the metal–metal distances achievable within the cryptand (Fig. 29).

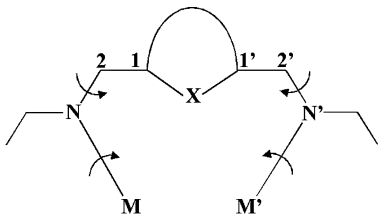

Fig. 29 Torsion angles in R3Bm and R3F head units.

The distance 2–2′ is essentially fixed, as are the X–1–2 and X–1′–2′ angles, however rotation about the bonds to nitrogen permits variation in the M–M′ distance and the twist of the cryptand strands. This rotation can be measured in terms of the torsion angles X–1–2–N and 1–2–N–M (and their equivalents on the other side). The 2–2′ distances for the phenyl and furan head groups can be calculated using molecular mechanics[45] as 5.135 and 4.908 Å, respectively, leading to minimum N–N′ distances of 5.361 and 5.435 (if the structure were planar). The planar arrangement, however, would bring the metal ions unreasonably close together (2.032 and 2.168 Å) so some twist is always observed. The range of torsion angles is restrained by the relationship between the three strands making up the cryptand (each must connect to the bridgehead on the axis of the crypt) as well as by the geometric preferences of the metal ions. The situation is further complicated by the possibility of *R* or *S* configuration at the amine nitrogen atoms; and by the observation that the three strands rarely have identical conformations. These contributions make it difficult (and probably fruitless) to model the system in detail.

That molecular mechanics calculations let both systems cover much the same range of M–M distances implies that the difference between the systems is not mechanical: the difference in M–M distance in cascade complexes of R3Bm and R3F cannot be explained in terms of the geometry at the head group. The two oxalate cryptates (Figs. 19 and 20) of the hexaprotonated ligands show that the two ligands are capable, at least when protonated, of adopting very similar cavity dimensions to accommodate a given anionic guest.

The question of cavity size in this pair of ligands has also been considered[41] by Fabbrizzi, who attributes the relative behaviour of the cryptand hosts to the capacity in R3F of "each NH–CH_2–C–O group to behave as a spring which can be operated through the variation of the magnitude of the corresponding dihedral angle", a mechanism apparently unavailable to the R3Bm (or the thiophene-linked R3S) analogue, in aqueous solution. The Pavia group have been involved in quantitative solution measurements, monitoring colour change on anion uptake, in ternary "cascade" systems, where the largest binding constants for these cryptate hosts are noted[40,46] with the strongly binding N-donor anions azide and cyanate, whose collinearity with the transition cations in the host had been established[18,47] by X-ray crystallographic or ESR studies. Treatment of hydrogen carbonate ion with the dicopper cryptate of R3Bm, but not R3S, generates another strongly bound ternary complex, whereas use of formate, acetate and nitrate generates only weak and rather similar binding constants.

8 Potential applications of oxoanion complexation by azacryptand hosts

There are many applications from the fields of catalysis, monitoring, recognition and transport which may be envisaged using these systems. The area of cascade catalysis, discussed earlier, holds promise but is still in its infancy. In the second area, the group of Fabbrizzi has been quick to exploit the possibilities of selective complexation of anions in cascade mode by the cryptate ligands while signalling *via* the fluorescence response from an intrinsic or extrinsic fluorophore. A recent review[48] from this group should be consulted for developments in this area.

In the field of binding and extraction of target oxoanions, work is underway[25,49] to exploit the selective recognition of particular anions by cage ligands. In particular combinations of host and guest, the enhancement of non-aqueous solubility generated by reduction of charge or attainment of charge-neutrality is effective in extraction and transport processes. However as most target anions have charges of −1 or −2, this requires that the host should function effectively at relatively low protonation levels. In one study designed to identify potential binding agents for the radiolabelled medically diagnostic and/or therapeutic pertechnetate or perrhenate anions at near-physiological pH, liquid–liquid extraction techniques were used to characterize the binding and distribution behaviour of complexes formed with azacages bearing secondary amino or amido functions. Clean 1:1 complex formation was observed and the most effective extraction was achieved[49] with oxooazacages derived by combination of triethanolamine with trencaps *via o*- or *m*-xylyl spacers. pH-dependence of extraction efficiency correlates with both lipophilicity and basicity of the ligands. Table 6 shows how this efficiency varies across a range (Fig. 30 of podand, *N*-methylated and unmethylated cryptand hosts). High lipophilicity is a prerequisite for good extractability but for good complexation of anions it must be accompanied by reasonable basicity. The methylated cryptand, Me_6R3Bm, synthesised *via* functionalisation of the Schiff-base-derived aminocryptand R3Bm demonstrates enhanced lipophilicity together with only slight lowering of basicity and represents a promising oxoanion complexant. Preliminary data on R3P suggests that its acidity is also enhanced upon methylation. Extraction experiments demonstrate that Me_6R3P is the most effective extractant for perrhenate and pertechnetate in the hexaaminocryptand series so far (Table 6). We were surprised to note that some podand complexants incorporating *tris*-aromatic substituents, particularly 2-napthyl, were superior extractants to both the methylated cryptand, Me_6R3P and to the successful oxoaza cryptand. The superior extraction behaviour of these podands presumably derives from their higher lipophilicity.

Few crystal structures have been obtained at the relatively low protonation levels involved in extraction studies at near-neutral pH and those that were obtained [49] (Fig. 31) showed the

Table 6 Extractabilities of pertechnetate and perrhenatewith azacages L^1–L^4 and tripodal counterparts L^5–L^{12} [$NaTcO_4$] or [$NaReO_4$] = 10^{-4} M; pH 7.4 (HEPES/NaOH buffer); [ligand] = 10^{-3} M in $CHCl_3$; shaking time 30 min.; T = 23 ± 1 °C[a]

Extractability (%)	L^{1b}	L^{2b}	L^{3b}	L^{4a}	L^{4b}	L^5	L^6	L^8	L^9	L^{10}	L^{11}	L^{12}
ReO_4^-	13	12	16	10	20		22					
TcO_4^-				14		21	26	20	8	47	16	3

[a] L^{1b} = Me_6R3Bp, L^{2b} = Me_6R3Bm, L^{3b} = Me_6R3F, L^{4b} = Me_6R3P; see Fig. 31 for L^5–L^{12}

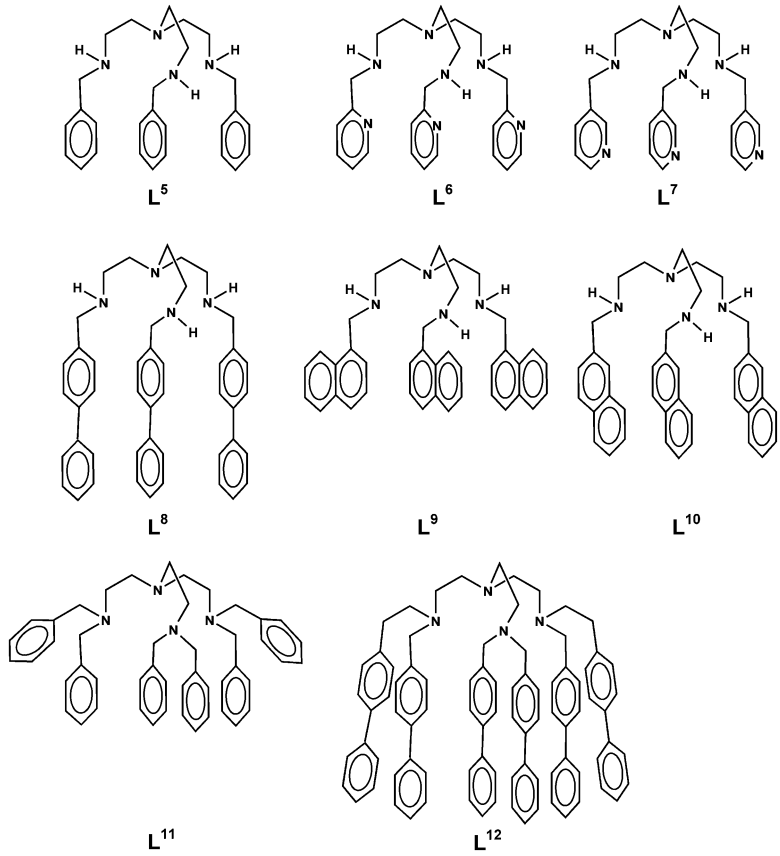

Fig. 30 Podand ligands used for selective transport experiments.

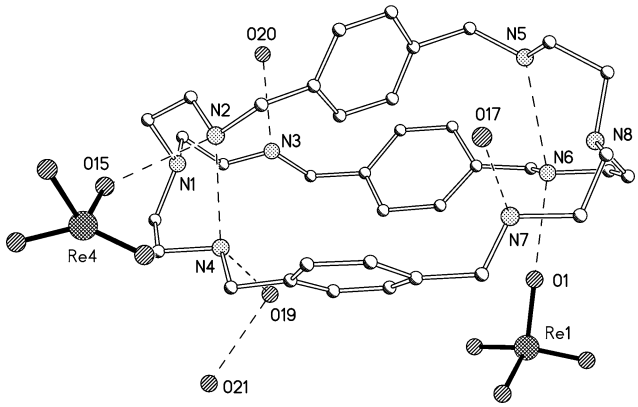

Fig. 31 Structure of $H_2R3Bp(ReO_4)_2 \cdot 4H_2O$: note two H-bonds crossing the cavity.

mononegative anion bound outside the cryptand cavity. It will be a matter of high priority in progressing this anion cryptate work to accumulate structural data in order to establish any correlation between cryptand conformation and protonation level. This may enable generalisations about the extent to which target anions are excluded at low protonation levels. A combination of NMR spectroscopy at defined pH and computer modelling would be helpful in supplementing X-ray crystallographic work. Finally the completion of calorimetric studies on at least some typical systems will enable analysis of the relative importance of enthalpic and entropic contributions to complexation constants.

9 Conclusions

• Oxoanion complexation measurements using protonated cryptate ligands show a thermodynamic "Cryptate effect", of at least one log unit *versus* analogous macrocyclic hosts, for complexation of mononegative anions, and of several log units for dinegative analogues.

• Crystal structures involving hexa-protonated hosts show tetrahedral and trigonal oxoanions are held mainly in cavity-bound sites for *m*-xylyl and 2,5-furano linked cryptands R3Bm and R3F, the anions retaining remnants of their hydration sphere which are involved in host–guest interaction *via* hydrogen bond bridging between guest and host.

• A clear charge-based selectivity is demonstrated between mono- and di-negative oxoanions of similar geometry.

• An important shape selectivity effect, including C=O to π stacking, is demonstrated for oxalate. This is associated with the largest stability constants so far reported for oxalate complexation, so large that the protonated host competes successfully for cation coordination of the oxalate ligand.

• In the 2,6-pyridine-spaced host R3P, the cleft-binding conformation (structurally demonstrated for both unprotonated and hexaprotonated forms of the ligand) often generates respectably large complexation constants especially at lower protonation levels, although it seems likely that this may be at the expense of selectivity.

• In the case of the oxalate cryptate of R3P, the relatively open cryptate conformation permits the protonation of one partially encapsulated anion, and the formation of a very strong, possibly symmetric, hydrogen bond linking a pair of oxalate cryptates in a dimeric arrangement.

• Other oxoanion cryptates of the pyridino-spaced host incorporate π stacking segments, such as nitrate intercalation between pyridine rings.

• In ternary complexation of oxoanions by ditransition ion cryptates, "cascade" reactivity is demonstrated *via* the formation of carbonate esters upon insertion of CO_2 into an M–OR bond transiently formed within the cryptate R3Bm.

The criteria established in this work regarding charge and shape selectivity in these cryptate hosts should assist investigation of complexation and reactivity of other important systems.

The indications that protonation equilibria of multiply charged anions are disturbed *via* charge selectivity effects in the presence of the cryptand host, may offer a basis from which to develop applications in selective transport and recovery, or removal of harmful or valuable multiply charged target anions.

10 Acknowledgements

JN thanks University of Canterbury NZ, and the Erskine Fund for facilities and support which enabled the preparation of this review. She thanks Professor Kip Powell for valuable discussions. RMT thanks the trustees of the Analytical Chemistry Trust Fund of the Royal Society of Chemistry for a SAC Research Studentship.
We thank the EPRSC mass spectrometry service in Swansea for results which have been most valuable in the early stages of the work and also for access to station 9.8 at Daresbury Laboratory.
The work of the graduate students who laid the foundation of this work, Dr Josie Hunter, Dr Beatrice Maubert, Dr David Farrell, and particularly that of Dr Grace Morgan and Dr Ibolya Pál, is gratefully acknowledged.
Coworkers and colleagues Professor Françoise Arnaud-Neu (CNRS Strasbourg), Dr Charles Harding, (Open University, Milton Keynes), Dr Woody Nieuwenhuyzen, (Queen's University Belfast), Professor Michael Hynes, (NUI Galway), and the group of Professor Karsten Gloe, (TU Dresden) are also thanked for their valuable input.

References

1 J.-M. Lehn, *Pure Appl. Chem.*, 1978, **50**, 871 and references therein.
2 B. Dietrich, *Pure Appl. Chem.*, 1993, **65**, 1457and references therein.
3 B. Dietrich and M. W. Hosseini in *Supramolecular Chemistry of Anions*, eds. A. Bianchi, K. Bowman-James and E. Garcia-España, Wiley-VCH, NY, 1997, pp. 45–62.
4 M. W. Hosseini, in *Supramolecular Chemistry of Anions*, eds. A. Bianchi, K. Bowman-James and E. Garcia-España, Wiley-VCH, NY, 1997, pp. 421–448.
5 J. Scheerder, J. F. J. Engerberson and D. N. Reinhoudt, *Rec. Trav. Chim. Pays-bas*, 1996, **115**, 307; F. P. Schmidtchen and M. Berger, *Chem. Rev.*, 1997, **97**, 1609.
6 H. E. Simmons and C. H. Park, *J. Am. Chem. Soc.*, 1968, **90**, 2431.
7 F. P. Schmidtchen, *Chem. Ber.*, 1981, **114**, 597.
8 D. Heyer and J.-M. Lehn, *Tetrahedron Lett.*, 1989, **27**, 5869.
9 J.-M. Lehn, R. Meric, J.-P. Vigneron, I. Bkouche-Waksman and C. Pascard, *J. Chem. Soc., Chem. Commun.*, 1991, 62.
10 B. Dietrich, J. Guilhem, J.-M. Lehn, C. Pascard and E. Sonveaux, *Helv. Chim. Acta*, 1984, **67**, 91.
11 M. W. Hosseini and J.-M. Lehn, *Helv. Chim. Acta*, 1988, **71**, 749.
12 P. Arranz, A. Bencini, A. Bianchi, P. Diaz, E. Garcia-Espana, C. Giorgi, S. V. Luis, M. Queroi and B. Valtancoli, *J. Chem. Soc., Perkin Trans.*, 2001, 1765.
13 B. Dietrich, M. W. Hosseini, J.-M. Lehn and R. B. Sessions, *J. Am. Chem. Soc.*, 1981, **103**, 1282.
14 M. W. Hosseini and J.-M. Lehn, *J. Am. Chem. Soc.*, 1982, **104**, 3525.
15 Q. Lu, R. J. Moteikaites, J. J. Reibenspies and A. E. Martell, *Inorg. Chem.*, 1995, **34**, 4958 and references therein.
16 A. E. Martell and R. J. Moteikaitis, *J. Am. Chem. Soc.*, 1988, **110**, 8059.
17 R. J. Motekaitis and A. E. Martell, *Inorg. Chem.*, 1992, **31**, 5534.
18 J. Nelson, G. G. Morgan and V. McKee, *Prog. Inorg. Chem.*, 1998, **47**, 167.
19 I. Pál, Ph.D. Thesis, Queen's University of Belfast, 2002.
20 T. Clifford, A. Danby, J. M. Llinares, S. Mason, N. W. Alcock, D. Powell, J. A. Aguilar, E. Garcia-Espana and K. Bowman-James, *Inorg. Chem.*, 2001, **40**, 4710.
21 G. G. Morgan, J. Nelson and V. McKee, *Chem. Commun.*, 1995, 1649.
22 G. G. Morgan, Ph.D. Thesis, Open University, 1991 ; A. A. Varnek, G. Wipff, A. S. Glebov and D. Feil, *J. Comput. Chem.*, 1995, **16**, 1.
23 V. McKee and G. G. Morgan, *Acta Cryst.*, 2003, **C59**, 150.
24 J. Dilworth and S. Parrott, *Chem. Soc. Rev.*, 1998, **27**, 43.
25 D. Farrell, K. Gloe, K. Gloe, G. Goretzki, V. McKee, M. Nieuewenhuyzen, J. Nelson, I. Pál, H. Stephan, R. M. Town and K. Wichmann, *Dalton Trans.*, 2003, 1961.
26 S. Mason, T. Clifford, L. Seib, K. Kucxera and K. Bowman-James, *J. Am. Chem Soc.*, 1998, **120**, 8899.
27 M. J. Hynes, B. Maubert, V. McKee, R. M. Town and J. Nelson, *J. Chem. Soc., Dalton Trans.*, 2000, 2853.
28 M. J. Hynes, *J. Chem. Soc., Dalton Trans.*, 1993, 311.
29 F. Arnaud-Neu, S. Fuangswasdi, B. Maubert, J. Nelson and V. McKee, *Inorg. Chem.*, 2000, **39**, 573.
30 B. Dietrich, J. Guilheim, J.-M. Lehn, C. Pascard and E. Sonveaux, *Helv. Chim. Acta.*, 1998, **67**, 91.
31 A. Bianchi and E. Garcia-España, in *Supramolecular Chemistry of Anions*, eds. A. Bianchi, K. Bowman-James and E. Garcia-España, Wiley-VCH, NY, 1997, pp. 217–276.
32 J. Nelson, V. McKee, B. Maubert, I. Pál and R. M. Town, *J. Chem. Soc., Dalton Trans.*, 2001, 1395.
33 J. L. Sessler, P. I. Sansom, A. Andrievesky and V. Kral, in *Supramolecular Chemistry of Anions*, eds. A. Bianchi, K. Bowman-James and E. Garcia-España, Wiley-VCH, NY, 1997, pp. 355–420.
34 L. O. Abouderbala, W. J. Belcher, M. G. Boutelle, P. J. Cragg, J. Dhaliwal, M. Fabre, J. W. Steed, D. R. Turner and K. J. Wallace, *Chem. Commun.*, 2002, 358.
35 P. D. Beer, M. G. B. Drew, D. Hesek and K. C. Nam, *Organometallics*, 1999, **18**, 3933.
36 J. Nelson, M. Nieuwenhuyzen, I. Pál and R. M. Town, *Chem. Commun.*, 2002, 2266.
37 F. Arnaud-Neu, R. M. Town and J. Nelson, work in progress.
38 B. A. Moyer and P. V. Bonnesen, in, *Supramolecular Chemistry of Anions*, eds. A. Bianchi, K. Bowman-James and E. Garcia-España, Wiley-VCH, NY, 1997, pp. 1–44.
39 J.-M. Lehn, *Pure Appl Chem.*, 1978, **50**, 871.
40 V. Amendola, L. Fabbrizzi, C. Mangano, P. Pallavicini, A. Poggi and A. Taglietti, *Coord. Chem. Rev.*, 2001, **219**, 821 and references therein.
41 V. Amendola, E. Bastianello, L. Fabbrizzi, C. Mangano, P. Pallavicini, A. Perotti, A. M. Lanfredi and F. Ugozzoli, *Angew. Chem.*, 2000, **39**, 2917.
42 Y. Dussart, C. Harding, P. Dalgaard, C. McKenzie, R. Kadirvelraj, V. McKee and J. Nelson, *J. Chem. Soc., Dalton Trans.*, 2002, 1704.
43 Y. Dussart, C. J. Harding, V. McKee and J. Nelson, XXIV ISMC Barcelona, 1999: to be published.
44 B. Kersting, *Angew. Chem. Int. Ed.*, 2001, **40**, 3987.
45 HyperChem Lite release 1.0 for Windows. Hypercube Inc., Gainsville FL. 1996.
46 V. Amendola, L. Fabbrizzi, C. Mangano, P. Pallavicini and M. Zema, *Inorg. Chim. Acta*, 2002, **337**, 70.
47 C. J. Harding, F. E. Mabbs, E. J. L. MacInnes, V. McKee and J. Nelson, *J. Chem. Soc., Dalton Trans.*, 1996, 3227; A. Escuer, C. J. Harding, Y. Dussart, J. Nelson, V. McKee and R. Vicente, *J. Chem. Soc., Dalton Trans.*, 1999, 223.
48 L. Fabbrizzi, M. Licchelli, G. Rabaioli and A. Taglietti, *Coord. Chem. Rev.*, 2000, **205**, 85 and references therein.
49 H. Stephan, K. Gloe, W. Kraus, H. Spies, B. Johannsen, K. Wichmann, D. K. Chend, P. K. Bharadwaj, U. Müller, W. M. Müller and F. Vögtle, in *Anions Separations: Fundamentals and Applications*, eds. R. P. Singh and B. A. Moyer, Kluwer, New York, 2003, in press.